Control and Evaluation of Stair Ascent with a Powered Transfemoral Prosthesis

By

Elissa Danielle Ledoux

Thesis

Submitted to the Faculty of the

Graduate School of Vanderbilt University

in partial fulfillment of the requirements

for the degree of

MASTER OF SCIENCE

in

Mechanical Engineering

August, 2016

Nashville, Tennessee

Approved:

Michael Goldfarb, Ph.D.

Thomas J. Withrow, Ph.D.

Karl E. Zelik, Ph.D.

To all transfemoral amputees, especially Richard, Ethan, and Pete.

ACKNOWLEDGEMENTS

The first credit goes to God, for placing me at Vanderbilt and carrying me through this experience. Next, I would like to thank my parents Marcus and Jennifer Ledoux, siblings Grace, Madelyn, Daniel, Catherine, Anne Marie, and Jonathan, grandparents, and relatives too abundant to list, for praying me through it.

Thanks goes to my research advisor, Dr. Michael Goldfarb, for providing the hardware, paying the amputee test subjects, and allowing me to work in his lab. I would like to thank him and the other members of my committee, Dr. Tom Withrow and Dr. Karl Zelik, for their advice on this project. I am also quite grateful to the members of the Center for Intelligent Mechatronics for creating a pleasant working environment and peaceably enduring the incessant buzzing of the $K4b^2$ metabolics system.

Next, I must absolutely thank my hardware support team, without whose timely help this project might have dragged on forever. Don Truex and Dr. Brian Lawson provided their expertise on electronics and code, while Drs. Jason Mitchell and David Comber helped fix the mechanical failures on countless occasions. These men have been a real blessing, resurrecting my morale in addition to the hardware. Thanks to them, I am not going to die behind my computer and a broken robot leg.

I am very thankful for all the Vanderbilt affiliates who have contributed to my emotional well-being, especially Drs. Tom Withrow, Brian Lawson, and Alex Pedchenko for their understanding and heartfelt encouragement throughout this journey. I sincerely appreciate Brian's alter ego as a guidance counselor, without whom my first year especially would have been a maze in the dark. And my senior design council buddies Tom and Alex have been a second family, preserving me from physical and emotional atrophy behind the digital screen. For those of you who told me I was good enough even when affairs indicated otherwise, I am eternally grateful.

Finally, I would like to thank the amputee test subjects, Richard, Ethan, and Pete, for sticking with me to the end as we literally climbed this mountain. Without them, this work would not have been possible.

TABLE OF CONTENTS

APPENDICES

LIST OF TABLES

LIST OF FIGURES

CHAPTER I

INTRODUCTION

1. Background

Amputation affects millions of people worldwide. In the United States alone, two million people live without one or more limbs [1]. Of these, 18.5% are transfemoral amputees [2]. Missing both the knee and the ankle joints poses significant locomotive obstacles, as shown in Figure I-1. Activities such as walking and stair ascent become difficult or even impossible to accomplish in a normal fashion. Healthy joints store, produce, and dissipate energy at different times in the gait cycle depending on the activity performed. During walking, the ankle provides active power at pushoff, while the knee primarily dissipates energy. During stair ascent, however, both joints produce net positive power: at knee extension, to raise the climber over the step, and at ankle plantarflexion, to push off. Activity of both joints is crucial for normal gait.
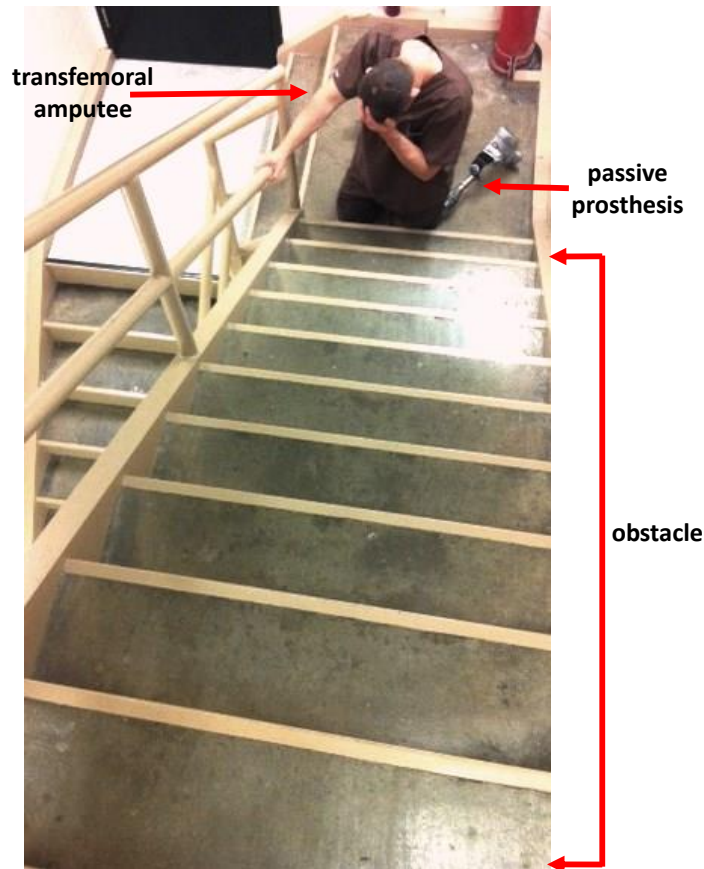
Figure I-1: Hindrance to Locomotion

While current lower limb prostheses meet amputees' basic needs, passive prosthetic devices cannot fully reproduce healthy limb motion. This is because they cannot produce net positive power, only store and return or dissipate energy. As a result, an amputee compensates for this reduced function using the rest of his body, which can lead to asymmetric gait, instability, increased stress on the sound limbs, and additional physical problems later in life [3]. Transfemoral amputees expend over twice as much energy on average as healthy individuals during level walking, where the ankle contributes most of the energy during the gait cycle [4]. For stair ascent,

1

similar or worse results can be expected because the knee joint is also active. Since a passive prosthetic knee cannot provide the active torque required to straighten the prosthesis and raise the amputee over the stair, the transfemoral amputee uses a step-to gait: stepping up stairs with his sound leg and bringing his prosthesis to meet it. Thus, ascending stairs becomes time-consuming and exhausting.

Prostheses with actively powered joints should be able to combat these issues. By controlling the joints to behave as virtual springs and dampers, energy can be introduced into the system, theoretically making gait easier (lower metabolic cost) and more natural (appropriate biomechanics) for amputees. However, powered prosthetics are generally much heavier than passive ones, and therefore might not supply enough power to overcome the effects of additional weight. No research apart from the author's work ([5, 6]) on transfemoral amputees has been done in the field to assess the benefits of powered prosthetics on the energy cost associated with amputee stair ascent. While stair ascent kinematics have been investigated for this demographic, none of these studies ([7-9]) have involved published metabolic assessments. And while a few groups ([4, 10-16]) have conducted metabolic studies on transfemoral amputees, these have only covered level walking gait. Some studies on healthy individuals ([17-20]), one of which ([20]) involved asymmetric gait, have analyzed steady state metabolics or biomechanics. However, apart from the preliminary work of the author, previously published in [5], and more extensive work submitted for publication in [6], there has been no investigation of the effects of powered prostheses on the metabolic energy expenditure of stair ascent for amputees, and no detailed metabolic analysis of any people highlighting unsteady-state stair ascent.

This work describes the control and assessment of a powered transfemoral prosthesis for amputee stair ascent. The goals are to determine if using a powered prosthesis can make climbing easier and more natural for above-knee amputees. The primary study compares the metabolic energy expenditure of three transfemoral amputees ascending stairs with a powered prosthesis relative to their own passive daily use prostheses, analyzing the degree to which a powered prosthesis facilitates climbing. Furthermore, this study compares the biomechanics of stair ascent using the powered prosthesis to those of healthy individuals, thus quantifying the extent to which it makes climbing more natural. The powered prosthesis used in this study was developed at Vanderbilt and is described in Section I-3. This work describes the hybrid active-passive stair ascent controller and its experimental validation, and it presents a method for analyzing metabolic activity under transient conditions.

2. Commercial Prostheses

Lower-limb prostheses currently on the market are predominantly passive. A typical transfemoral prosthesis uses a carbon fiber spring ankle/foot combination and a microprocessor knee with modulated damping. Both of these joints are inherently passive. The spring ankle/foot can store and return energy of the user, while the knee can only dissipate energy; however, neither of these joints can produce net positive power, and therefore cannot adequately replicate healthy limb function. Following is an overview of commercial prostheses.

Ankles/Feet

Carbon-Fiber Spring Feet

Most ankle/foot prostheses are completely passive carbon-fiber springs of various stiffnesses. These strong and lightweight springs can be leaf or C-shaped. They store and release energy but do not provide active assistance or reproduce normal ankle/foot function at pushoff. Thus, they fundamentally cannot provide net positive energy to the user for propulsion in either walking or stair ascent. Examples of these devices are shown in Figure I-2.

Figure I-2: Standard prosthetic feet.
a) Ossur Vari-Flex b) Fillauer AllPro c) Otto Bock Triton d) Freedom Innovations Pacifica LP

Proprio Foot

The Ossur Proprio Foot, visible in Figure I-3, is a semi-active ankle unit. It modulates ankle position using a motor, causing the prosthesis to dorsiflex during swing phase and adapt its equilibrium angle to the ground slope during stance. It does not provide external power to the user and thus does not facilitate stair ascent.. The equilibrium position modulation allows amputees to wear shoes with various heel heights, a practice facilitated by insertable heel wedges. The prosthesis is made of an aluminum frame with a carbon-fiber leaf spring foot. It weighs 1.22 kg (2.69 lb) and can support a user up to 125 kg (276 lb). The motor is powered by a Li-ion battery with a 1-2 day charge life. [21]

Figure I-3: Ossur Proprio Foot

3

BiOM

The BiOM, in Figure I-4, is the only fully active ankle unit currently on the market. It provides powered pushoff to the user during walking or stair ascent activities. This external power is transmitted through a series elastic actuator consisting of a motor, ball screw and spring. The foot is a carbon-fiber leaf spring. The prosthesis has a 6-axis IMU for sensing acceleration and angular velocity, as well as encoders on the motor and joints to measure ankle position. It weighs 2 kg (4.4 lb), can support a 130 kg (287 lb) user, and is powered by a Li-poly battery with a life of 4-5000 steps. [22, 23]

Figure I-4: iWalk BiOM

Knees

Polycentric

The most basic type of knee prosthesis is a polycentric 4-bar knee, shown in Figure I-5. It is a passive, mechanical linkage that geometrically locks during stance and unlocks during swing. The changing kinematics cause the knee center to shift throughout the gait cycle. Due to its geometry and passive nature, such a knee would buckle if an amputee attempted to ascend stairs with it in a step-over fashion.

Figure I-5: Polycentric 4-Bar knee

C-Leg

The Otto Bock C-Leg, visible in Figure I-6a, is a common passive microprocessor knee prosthesis, the first to variably control both flexion and extension damping. Height adjustable between 289-534 mm, it weighs 1.24 kg (2.73 lb) and can support a user up to 136 kg (300 lb). It has a hydraulic damper at the knee, biased towards extension by a spring, and with both flexion and extension port orifices controlled separately by a single, rotary valve and motor. The valves can be open, partially or completely closed, allowing free swing, damping or locking. Since this joint only dissipates energy, it does not provide the active torque required for stair ascent. Hall Effect sensors measure knee angle and velocity, and strain gauges measure shank heel and toe loads. A microprocessor uses these signals to control damping for various gait states, including stance, swing, stair descent, and sitting. When the battery is low, the knee defaults to high damping. The C-Leg is weatherproof but not waterproof and will beep or vibrate for malfunctions. The default state upon malfunction is stance flexion damping. [24-26]

Rheo Knee

The Ossur Rheo Knee, in Figure I-6b, uses magnetorheological fluid to control damping at the knee joint. Magnetic particles align when a magnetic field is applied, increasing fluid viscosity, so the knee resistance is higher during stance and lower during swing. A constant power spring provides slight extension assistance, but not enough to enable normal stair ascent. The Rheo Knee has five sensors, one of which is a gyroscope, enabling speed adaptation. The controller can detect stance and swing gait phases in addition to level walking and stair descent activities. The unit is 236 mm tall, weighing 1.63 kg (3.59 lb), and it can support users weighing up to 136 kg (300 lb). The default knee state is free, but users can manually lock it in an extended position. [27]

Plie

The Plie (Figure I-6c), by Freedom Innovations, is a hydraulic and pneumatic microprocessor knee with two modes: stance and swing. Stance is high damping, while swing damping varies in inverse proportion to knee flexion angle. The default state is stance resistance. As with the other microprocessor controlled knees, the Plie is passive and does not assist with stair ascent. Control is based on load cell and knee angle sensor signals. The Plie 3 is waterproof (IP67 submersible for 30 min) and has a 24-hr minimum battery life. It weighs 1.24 kg (2.73 lb) and can support users weighing 125 kg (275 lb). [28]

Genium X3

The Genium X3 (Figure I-6d), by Otto Bock, is the top-of-the-line, microprocessor controlled prosthetic knee. It is waterproof with a 5-day battery life, weighs 1.9 kg (4.2 lb), and can support users weighing up to 125 kg (275 lb). This knee has six sensors: a single-axis gyroscope, a 2-axis accelerometer, a knee angle sensor, and force and torque sensors for the shank, knee and ankle. Information from these sensors can be used to control hydraulic knee damping during stance and swing phases of gait. Several activities are possible, including walking forward and backward on level ground and slopes, ascending and descending stairs, and running. While stair and slope ascent are not powered, the knee joint locks at a maximum flexion angle instead of collapsing. [29]

Figure I-6: Microprocessor knees.
a) Otto Bock C-Leg   b) Ossur Rheo Knee   c) Freedom Innovations Plie Knee   d) Otto Bock Genium X3

VGK

The VGK ("Very Good Knee"), shown in Figure I-7, is a variable damping hydraulic knee that uses microkinetic control. It requires no battery and is powered by fluid polymer decompression. This power is used to adjust a vortex valve and force fluid under the piston through it, increasing resistance under load (higher pressure swirls fluid against the valve walls) for stability. The stance resistance for the valve can be manually set to free, low, or high. The dissipative nature of this knee does not facilitate stair ascent. The VGK constantly adapts to load and gait speed changes and incorporates a stumble recovery feature. It is water resistant with a maximum user weight of 125 kg (275 lb). [30]

Figure I-7: Very Good Knee

6

Power Knee

The Ossur Power Knee, in Figure I-8, is the only actively powered commercial knee prosthesis. It has two basic modes: stance and swing, selected by ground contact. Standing mode (stance) is the default state. In stance, the knee straightens/locks, while in swing, it actively flexes and extends. This enables standing and stair ascent. Voluntary resistive knee flexion can be enabled in stance phase, so sitting and stair descent are possible activities. The Power Knee weighs 3.19 kg (7.1 lb) including the battery, which has a 12-hr operating life. [31, 32]

Figure I-8: Ossur Power Knee

3. Vanderbilt Powered Prosthesis

The Vanderbilt powered prosthesis, visible in Figure I-9 and described in [33] is an electromechanical prototype comprised of individually powered knee and ankle units. Each has magnetic encoders, one absolute (on the joint) and one incremental (on the motor) used to calculate angular position and velocity. An on-board embedded system houses a Microchip microcontroller, a custom-designed servo-amplifier, and a 6-axis inertial measurement unit, while a custom-designed magnetic load cell beneath the knee joint measures shank axial force. Both joints are driven by brushless DC motors. The knee's 200 W Maxon EC 30 4-pole motor is capable of supplying 85 N·m of torque at the joint through a 176:1 transmission ratio. The ankle's 100 W Maxon EC 60 flat motor can provide 110 N·m of joint torque through a 115:1 transmission ratio, while a carbon-fiber foot provides additional torque by means of a parallel spring engaged only in dorsiflexion. Designed to fit within the anthropometric weight and height envelope of a 20th percentile female, it weighs 5 kg (11 lb) and has a minimum build height of 492 mm (19.37", pyramid to ground, foot shell included). The main control code is programmed in C on the microcontroller and runs at 500 Hz, while a micro SD card holds tunable patient-specific parameters and logs sensor data. The prosthesis has several activity capabilities: sitting, standing on level ground and slopes, walking on level ground and slopes, ascending and descending stairs. The 24 V lithium-ion battery lasts approximately 1500 strides or 1.5 hrs of continuous walking. Additional publications and videos featuring this prosthesis, developed under the direction of Professor Michael Goldfarb, can be found on the Center for Intelligent Mechatronics laboratory website at http://research.vuse.vanderbilt.edu/cim/research_leg_pka.html.
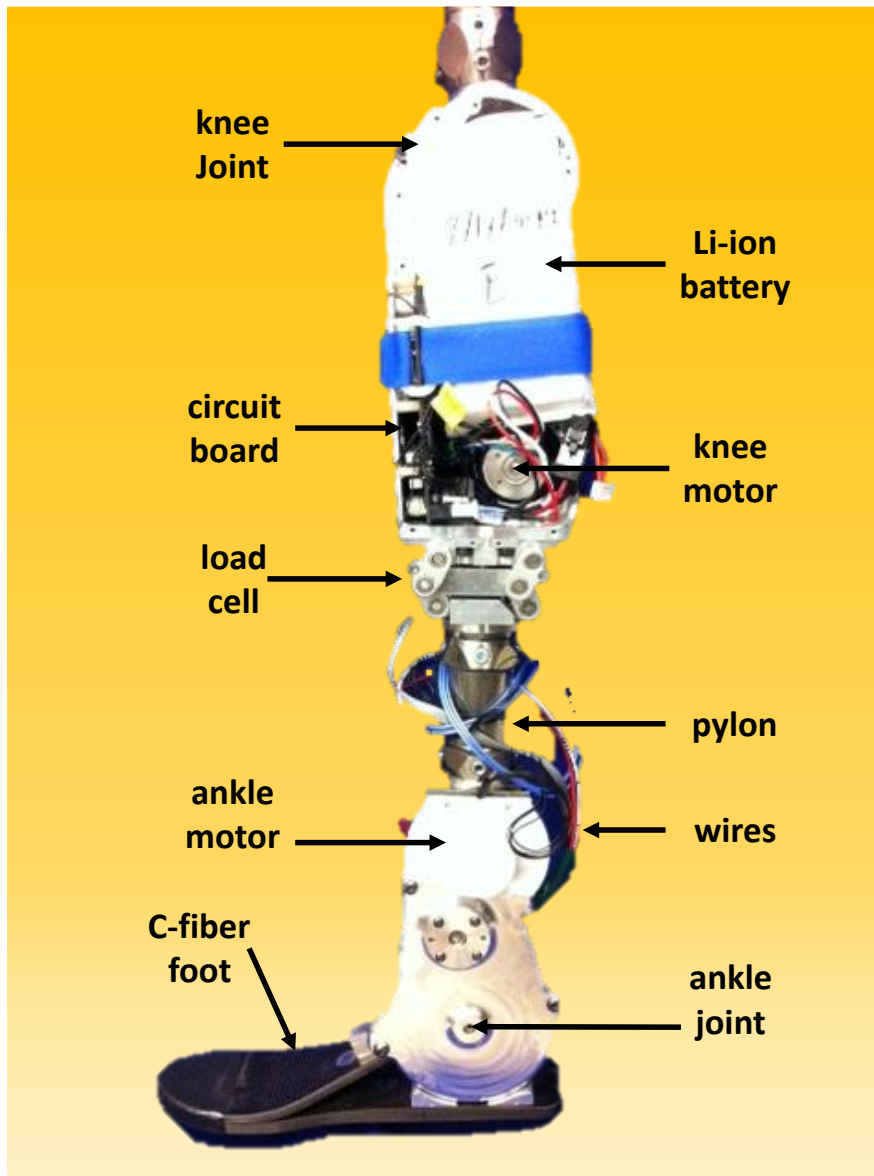
Figure I-9: Vanderbilt powered prosthesis

CHAPTER II

CONTROL AND TUNING

1. Control Scheme Overview

The powered prosthesis control is implemented through a three-tiered scheme: high-level activity selection, middle-level finite state machines, and low-level current commands. The main code is programmed onto the Microchip microcontroller in C, while patient-specific parameters are set on a micro SD card using a MATLAB graphic user interface (GUI).

The high-level activity controller, diagrammed in Fig. II-1, recognizes the user's intent through sensor signals in order to choose the correct activity to perform. Currently implemented activities are ground adaptive standing/sitting, variable cadence walking, and stair ascent and descent [5, 6, 8, 33, 34]. Because the testing protocol required the subjects to walk across a level floor and descend stairs in addition to ascending, the powered prosthesis also used level walking and stair descent controllers previously implemented by Lawson et al [8, 33]. Transitions between activities are described in Table II-1. For safety reasons, all activity transitions occur through standing mode, and all except the level walking entrance include minimum time constraints in order to reduce accidental activity changes.
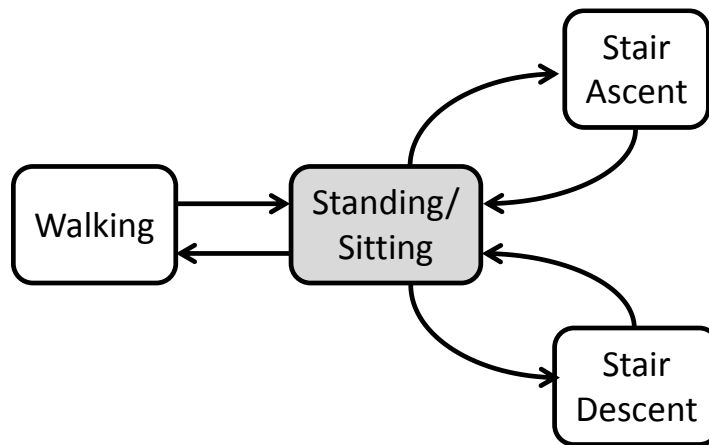
Figure II-1: Activity selection controller

Table II-1: Activity Transitions

Activity	Entrance	Exit
Stair Ascent	Thigh pointed backward No load	Thigh pointed down Passive state
Stair Descent	Thigh pointed forward No load	Thigh pointed down High load
Level Walking	Dorsiflexed ankle High load	Straight knee Low Load

The middle level controllers are activity-specific finite state machines. These controllers guide the prosthesis through a pattern of states, the number of which depends on the desired biomechanics for each activity. Piecewise passive impedance or hybrid active-passive control is the method of choice, using the law

$$\tau_j = k_j\left(\theta_j - \theta_{eqj}\right) + b_j\dot{\theta}_j \tag{1}$$

where τ specifies joint torque (controlled by commanding motor current), θ is joint angle, and $\dot{\theta}$ is joint velocity. The subscript j represents an individual state or transition for the specified joint. The virtual impedance parameters are k, b and θ_{eq}, where k is the spring constant, b is the damping coefficient, and θ_{eq} is the equilibrium position of the virtual spring. These parameters can be adjusted for each state in order to specify the desired joint torques and introduce positive power to the system. In passive impedance control, all impedance parameters remain constant within each state. In active trajectory control, while k and b remain constant, θ_{eq} is varied. Using a moving equilibrium angle and high gains distinguish active trajectory from passive impedance control. The benefits of using a hybrid approach are that fewer parameters are necessary for tuning, and resulting joint motions are smoother, due to the fewer number of states and gradually changing equilibrium angle. Although using a single state, and therefore a single trajectory, might achieve the most consistent motion, this method of control is undesirable from the user's perspective. In such a case, the prosthesis would be "driving" the amputee instead of working in accord with him, and transitions between gait phases would be out of his control. While the standing/sitting and stair descent controllers use purely passive impedance control [8, 34], stair ascent and walking use a hybrid active-passive combination [5, 6, 33]. These two controllers superimpose an additional torque pulse during the ankle trajectory at pushoff to provide an extra boost.

At the lowest level, the motors are controlled using current commands. The desired joint torques specified by the middle-level controller are adjusted to compensate for Coulomb friction inherent in each joint, as well as the torque contribution from the parallel spring at the ankle, engaged in dorsiflexion. The adjusted torques are converted to current commands using the equation

$$i = \frac{\tau}{\text{N} \cdot K_T} \tag{2}$$

where is τ joint torque, i is desired motor current, N is the transmission ratio, and K_T is the motor's torque constant, available from the data sheets.

2. Stair Ascent Controller

The state diagram, shown in Fig. II-2, comprises four states: *Straighten* (State 0), *Rollover* (State 1), *Step* (State 2), and *Bent* (State 3). The even numbered states are passive impedance based, while the odd ones are active trajectories between them. The stair ascent activity begins in *Step* (State 2), where the knee flexes to allow the amputee to position his prosthetic foot on the stair ahead of him. After completing the trajectories, the prosthesis immediately transitions into *Bent* (State 3). Upon receiving a load and experiencing slight ankle dorsiflexion, the prosthesis enters *Straighten* (State 0), a linear trajectory where the knee straightens to raise the amputee over the stair. Once the knee angle is below a certain threshold, the prosthesis has entered *Rollover* (State 1). It remains here while under load to allow the amputee to swing his sound leg onto the next stair. As he shifts weight to his sound side, the prosthesis transitions to *Step* (State 2). In this stepping motion, the knee and ankle trajectories are driven using cubic spline interpolation. The ankle plantarflexes to propel the amputee upwards, with torque supplemented by a superimposed current pulse, and then both joints flex as the amputee swings the prosthesis forward to land on the stair ahead. Completion of the trajectories indicates entrance into *Bent* (State 3), and the cycle continues.

The user can exit the stair ascent controller in two ways: weight-bearing (from State 1) if the user remains standing on the prosthesis for a specified time, and non-weight-bearing (from State 3) if the thigh is pointed downward for a specified time. The transitions between states and activities are summarized in Table II-1.
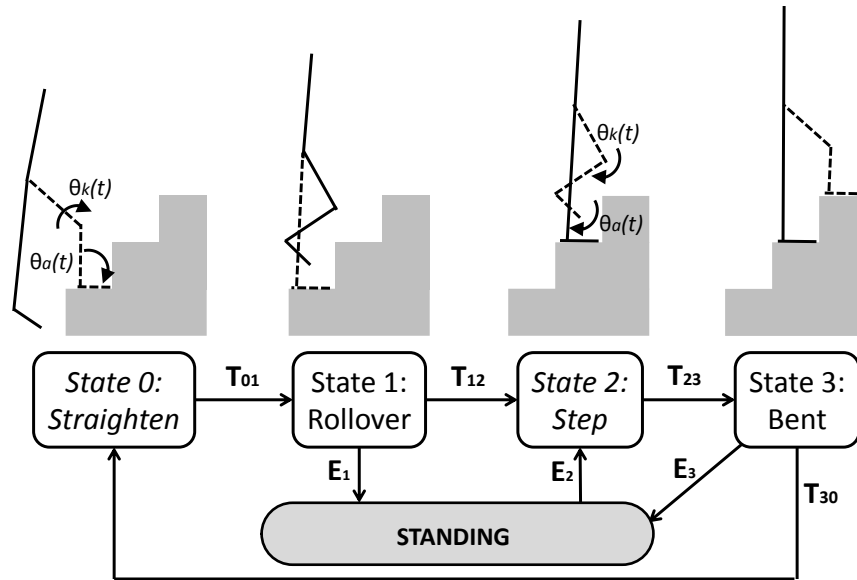
Figure II-2: Stair ascent controller. Italicized states are trajectories; other states are not.

Table II-2: Stair Ascent Controller Transitions

Transition	Conditions
T_{01}	Knee is straight Ankle is straight
T_{12}	Load is low
T_{23}	Trajectory completed
T_{30}	Load is high Ankle is dorsiflexed
E_1	Load is high Thigh is pointed down
E_2	Load is absent Thigh is pointed backwards
E_3	Load is absent Thigh is pointed down

Practically implementing this control philosophy in the code required three state functions. The first state, *Straighten* (State 0) is identical to the corresponding state described above. In this function, the knee equilibrium angle ramps from its initial high value to a low one in order to straighten the knee and raise the amputee over the step. Once the knee is straight, the code enters *Rollover* (State 1), which also corresponds to the identical state described previously. Here all impedance parameters are constant. Although the primary exit trigger is deloading the prosthesis, this state is held for a minimum time period of 0.1 s in order to prevent a premature transition to the next one. This reduces the likelihood of accidental triggers due to load imbalance or hesitation on the part of the amputee as he stands on the prosthesis and swings his sound leg forward. Once both conditions have been met, the controller switches to the State 2 function, called *Step* in the code and comprising both *Step* (State 2) and *Bent* (State 3) above. First, this function executes the joint trajectories corresponding to the stepping motion. Once complete, the final equilibrium positions of the flexed joints are held constant, implementing *Bent*. Since impedance parameters do not change here, no state-specific tuning is required, and it is not included in the user

interface described in Section II-3. The controller remains in this state until the load threshold is met to transition to *Straighten* (State 0) and continue the gait cycle. For the C code implementing this controller, see Appendix C.

3. User Interface

Each patient requires a unique set of controller parameters. These consist of the impedance parameters for the control equations, signal thresholds for transitioning between states and activities, and a few miscellanea. A new page was implemented in a pre-existing GUI for tuning the stair ascent parameters. This page is depicted in Fig. II-3.
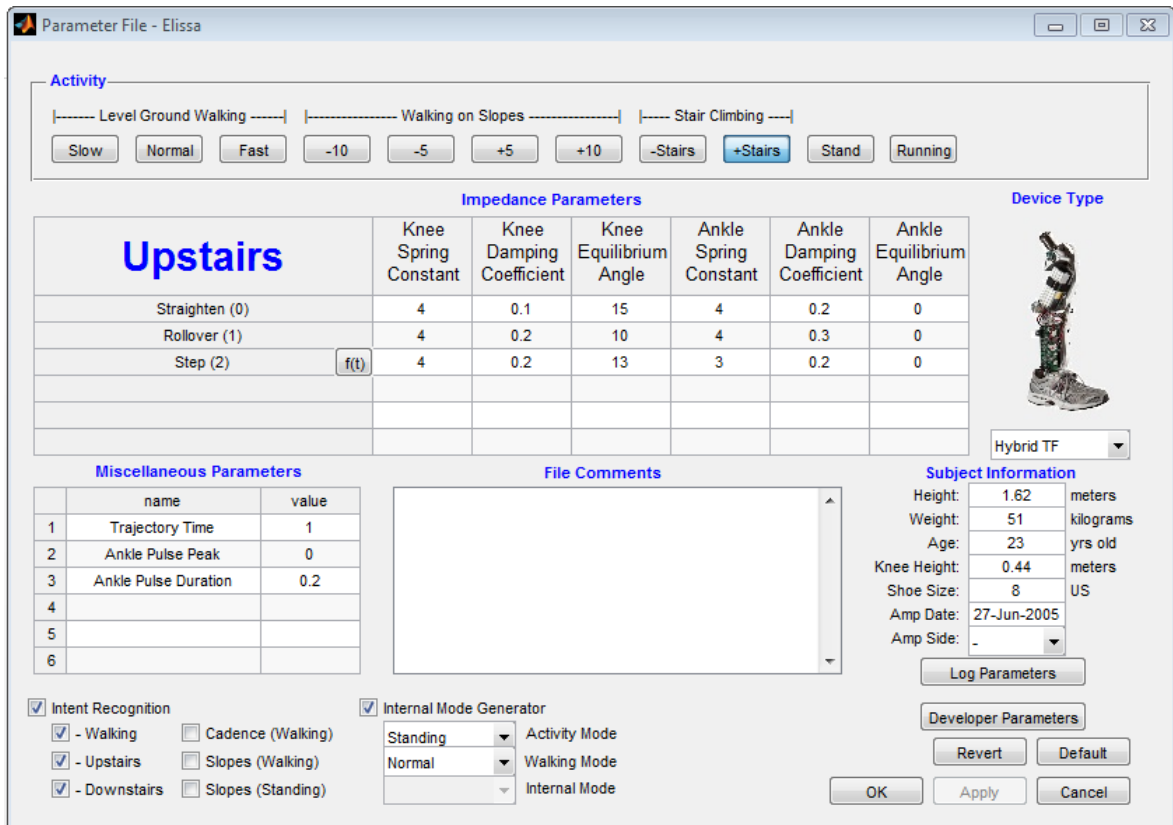
Figure II-3: Stair ascent activity page

The strip of buttons along the top of the window allows the user to select which activity parameters to tune. The "+ Stairs" button is highlighted, indicating that this page is for stair ascent. The main table in the middle of the window contains the impedance parameters for each state and each joint of the stair ascent controller. The user can type in values for these here. The "Default" button on the bottom right supplies recommended order of magnitude numbers as a starting point.

Clicking the "f(t)" button by State 2 brings up a new window for designing the joint trajectories in *Step* (State 2) for pushoff and swing. Shown in Fig. II-4, this is an interactive plot where the user can drag six specific points of each spline curve to adjust its trajectory. These curves are originally green and change to yellow when adjusted. The knee joint is the top trajectory, while the ankle joint is the bottom one. The horizontal axis represents percent of normalized trajectory time, while the vertical axis denotes joint angle in degrees. Clicking the "Restore" button sets the trajectories to match average healthy stair ascent biomechanics from Riener's data [17], and the "OK" button saves the curves and closes this window. "Cancel" closes the window without saving changes.
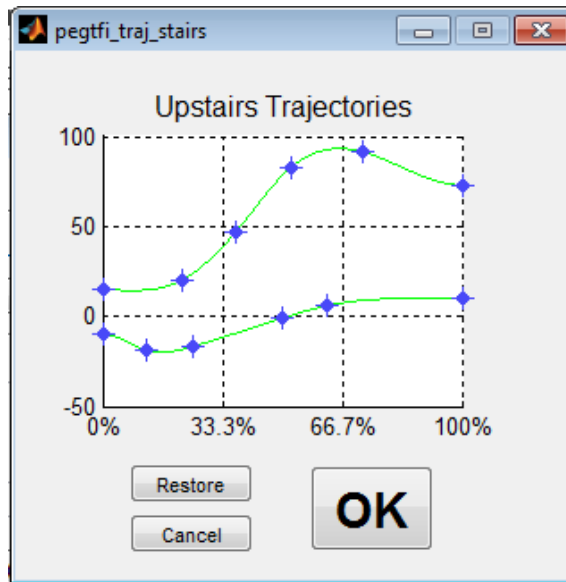
Figure II-4: Stair ascent trajectories

The table of miscellaneous parameters on the left side of the activity page allows the user to adjust the trajectory time in seconds as well as the amplitude and duration of the torque pulse in N·m and seconds, respectively, superimposed at the ankle joint for pushoff.

The "Developer Parameters" button opens a new window with a table holding a gamut of parameters specific to the prosthesis and the patient. Values can be typed in by the user. The most relevant parameters to the stair ascent controller are the signal thresholds for transitioning between states and activities, described in Section II-2. Clicking the "OK" button saves the parameter file to the micro SD card used in the prosthesis, while "Cancel" closes the file without saving changes. For the experiments described in Section III, a unique parameter file was created for each amputee. Once tuned, this set of parameters was used for all tests with the powered prosthesis for that subject.

4. Parameter Tuning

All controllers required subject-specific parameter tuning in order for the amputees to achieve biomechanically appropriate gait. The stair descent controller, described in [8], is purely passive impedance based. Because stair descent is primarily a power dissipating activity, kinetics were not a major concern, and this controller required little tuning in order to decently emulate healthy biomechanics from Riener et al. [17].

The level walking controller, explained in [33], uses the hybrid active-passive approach discussed above. This controller was tuned for variable cadence ambulation in order to enable the amputees to self-select their paces. Since the power transfer from the foot at pushoff is critical for biomechanically efficient gait, the most important parameters to adjust were the ankle angle threshold to trigger pushoff as well as the magnitude and duration of the extra torque pulse. These and impedance parameters were tuned for each subject to produce biomechanics representative of healthy walking from Winter [35].

Stair ascent controller tuning was the most time-intensive for several reasons. First, this controller was the one whose biomechanical and metabolic effectiveness was assessed. Secondly, both the knee and the ankle joints provide significant power transfer in different portions of the gait cycle. These joints must be coordinated to deliver this power at the appropriate times. If the timing and impedance parameters are not appropriate, the knee could collapse instead of straighten in stance, it could kick out early or pushoff could come after the prosthesis is in the air, or the toe could scuff the step. Any of these could result in a fall, causing damage to both the user and the hardware. Finally, because passive prostheses do not provide power at the knee joint, none of the amputees

13

were accustomed to ascending stairs in a step-over manner. Thus, they had to re-learn this motion, and at first had some difficulty coordinating their limbs and trusting the prosthesis with their weight. As the amputees acclimated, they began climbing faster and weighting the prosthesis more than the banister. Subjects trained 1-2 times per week, climbing approximately 25-40 flights per session over a period of 1.25-2 hours. This corresponds to approximately 10 consecutive weeks of training. However, interruptions in the training period, such as hardware failure or subject absence, extended these periods and required re-acclimation.

The most critical controller parameters to adjust were the transition trajectory times and positions (to enable a comfortable fixed pace), and the load thresholds for state transitions. The trajectories needed high gains due to the large torques required. Shorter amputees required higher knee and ankle flexion during the stepping trajectory and *bent* state than taller ones in order to achieve foot clearance over each stair and then allow the amputee to mount. Each subject climbed approximately 6,000-12,000 stairs throughout several training sessions before he was ascending comfortably with gait reflecting healthy biomechanics from Riener et al. [17]. Once an amputee had acclimated to the device and controller parameters had stabilized, official testing began.

CHAPTER III

EXPERIMENT 1: STAIR ASCENT CONTROLLER VALIDATION

1. Protocol and Data Acquisition

In order to determine the effectiveness of the transfemoral prosthesis in making climbing easier and more natural, stair ascent experiments were performed with three male amputee subjects. "Easier" was gauged by the prosthesis' ability to reduce metabolic energy expenditure, and "more natural" was quantified through joint biomechanics assessment.

For the metabolic data collection, pulmonary gaseous exchange rates of oxygen and carbon dioxide were measured using the COSMED K4b^2 indirect calorimetry system. The wearable apparatus, shown in Figure III-1, consists of a vest with the sensor unit and a battery, as well as a breath mask with a turbine and a sample line. The equipment measures the subject's O_2 and CO_2 ventilation rates in mL/s, with values reported approximately every 2-15 seconds. Data was stored on the testing unit during use and downloaded afterwards.
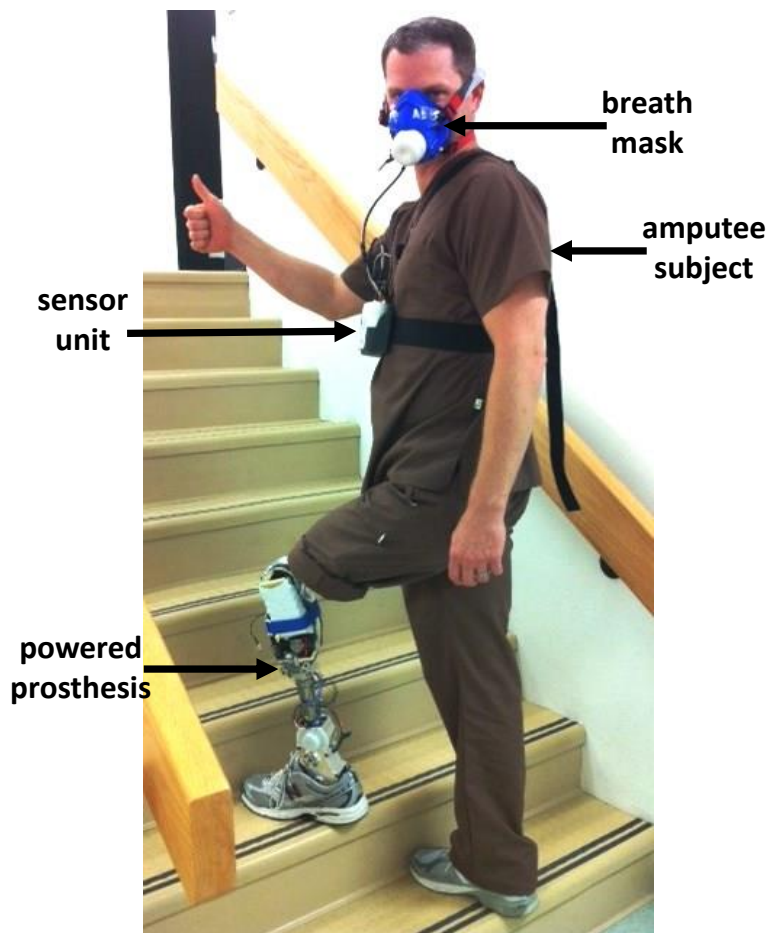
Figure III-1: Subject wearing metabolic apparatus.

Two different prosthesis conditions were tested: powered and passive. The powered case comprised active control of both the knee and ankle joints of the robotic prosthesis, using the controller described in Chapter II in order to produce positive power within the system. The passive test utilized the amputees' daily use prostheses, which were all variable damping knees with carbon-fiber spring feet.   The daily use prostheses were approximately half the weight of the powered prosthesis (~2.5 kg vs. 5 kg). Subject specifications are provided in Table III-1.

Table III-1: Subject Specifications

Subject	Age	Prosthesis	Amputation
1	46	C-Leg	4 yr
2	46	Plie	1 yr
3	43	VGK	9 yr

The powered and passive conditions were tested during four sessions per person in alternating orders. Subjects were instructed to avoid consuming energy drinks or cocaine before testing, as powerful stimulants can cause erratic metabolic activity. On the day of a testing session, a subject donned one of the prostheses and the metabolic apparatus. Following a brief calibration interval, he rested in a seated position for 3 minutes. Then he rose, walked to the stairwell (a distance of approximately 17 m), and ascended three flights of stairs totaling 79 steps. At the top, the amputee turned and descended the stairs, then returned to his seat and rested another 3 minutes to end the test. Times were recorded at each activity transition. After an additional rest period of approximately 15-20 minutes, the test was repeated with the other prosthesis. Although due to staircase limitations, the amputees did not reach steady state during the climbs, this protocol was deemed acceptable based on the fact that people rarely ascend more than three consecutive flights of stairs anyway.

This study was approved by the Vanderbilt University Institutional Review Board. Prior to their involvement, the amputee subjects read and signed informed consent documents. They were allowed to withdraw from the study at any time.

2. Analysis

A. *Joint Biomechanics Analysis*

Kinematic and kinetic data, consisting of angles, speeds, torques, and powers, were measured and logged on the prosthesis as in [33], using the encoders, embedded system, and a micro SD card. Joint angles and angular velocities were calculated via encoders, whereas joint torques were estimated using motor currents and the known and/or estimated passive characteristics of the prosthesis (motors and transmissions, frictions and foot spring). Powers were found by multiplying joint torques and velocities. Because the amputees paused for about 15% of stride time at the end of each stride with the powered prosthesis, making trajectories appear phase shifted, these static periods have been removed for the purpose of accurate kinematic and kinetic comparisons. The pause, according to the subjects, is due to the fact that they are not used to trusting the prosthetic side and so hesitate to weight it.

B. *Transient Metabolic Analysis*

Oxygen and carbon dioxide gaseous exchange rates were collected during the aforementioned testing sessions. All data was exported from the COSMED K4b^2 software and post-processed in MATLAB (see Appendix D for this code). Due to the uneven sampling rate and scattered measurements, the data required filtering. First, a 5-point median filter was applied in order to reduce scatter. Then, to evenly discretize the signals, the data were resampled at 100 Hz using linear interpolation. After resampling, a zero phase filter was applied in the following manner to eliminate noise. First, a discrete Fourier transform was taken, then the high frequency content (above 0.01 Hz) was removed, and an inverse Fourier transform was applied to return the data to the time domain. Finally, the data were downsampled at a rate of 0.5 Hz to improve calculation speed. After filtering, the data were body-mass normalized. A representative plot for the powered prosthesis is shown in Figure III-2, depicting the discrete data points for oxygen and carbon dioxide exchange recorded by the instrument

and body-mass-normalized, as well as the filtered curves obtained therefrom. The shallow portion in the beginning is the resting baseline, and the highlighted region is the stair ascent period. The reason the curves begin to rise before stair ascent initiation is that the amputees were walking into the stairwell.
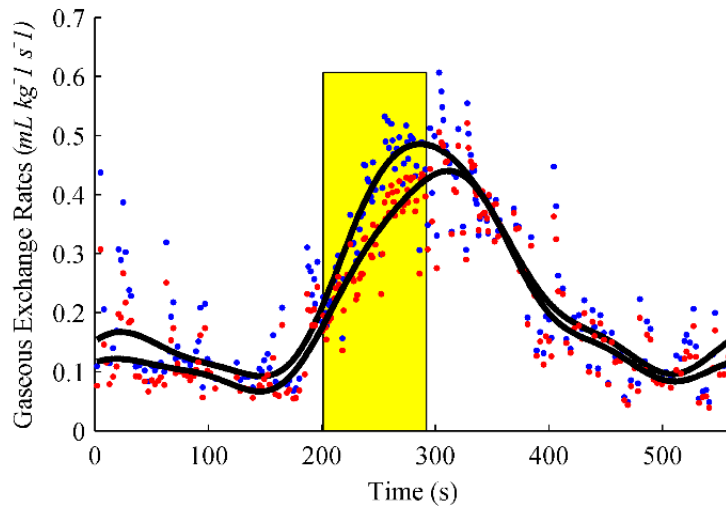
Figure III-2: Gaseous exchange rates with the powered prosthesis. The blue dots represent oxygen, and the red dots show carbon dioxide. The black curves are the filtered data.

Because the amputees did not reach metabolic steady state during their climbs, the respiratory gases peaked at different times and sometimes before or after the subject reached the top of the stairs. For this reason, an appropriate activity time needed to be determined (see Appendix E for more details). In order to do this, the metabolic power for each trial was determined using a formula based on the work by Brockway et al., 1987 [36]:

$$\dot{E} = 16.58\dot{V}_{O_2} + 4.51\dot{V}_{CO_2} \tag{3}$$

where $\dot{V}_{O_2}$ and $\dot{V}_{CO_2}$ are the body-mass normalized, gaseous exchange rates of oxygen and carbon dioxide, respectively, in mL/(kg·s). The coefficients are proportional to the metabolic energy obtained from nutrient consumption [36]. The time to peak power was found from this curve. The end time for the activity period, t_f, was selected as the time to either ascent completion (rise time, t_r) or peak energy rate (peak time, t_p), whichever was longer if the two did not coincide. A power curve with these times indicated is shown in Figure III-3.
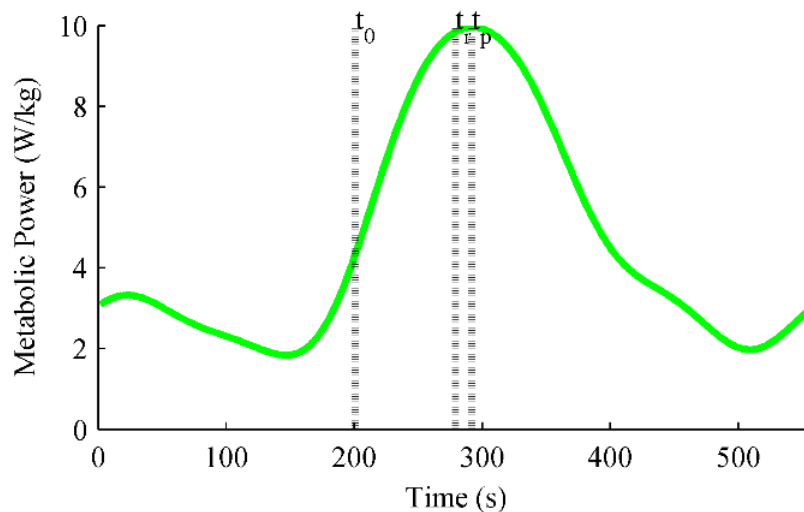
Figure III-3: Metabolic power

In order to compare effort level between the two test conditions, metabolic energy expenditure E (J/kg) was calculated as a function of the area under the power curve. This measure was chosen for analysis because it combines the respiratory exchanges of oxygen and carbon dioxide, presenting a more holistic representation of effort than only oxygen consumption would. It was found from the respiratory gas measurements by integrating the area under the power curve for the activity period:

$$E = \int_{t_0}^{t_f} \dot{E} \, dt \tag{4}$$

The variable t represents time, where t_o indicates the time stair ascent initiated, and t_f represents the activity completion time determined above. The metabolic power was averaged over the stair ascent and initial rest periods, and the resting baseline was subtracted from the stair ascent duration. The resulting rate was then multiplied by the activity time span to determine net metabolic energy cost for ascending the stairs.

Average respiratory exchange ratio R (also known as "respiratory quotient") was also calculated for each trial in order to determine whether the ascent was aerobic or anaerobic. This quantity is the ratio of carbon dioxide to oxygen respired, where 0.85-1.0 is the threshold between aerobic and anaerobic activity. Values above 1.0 are anaerobic, and values below 0.85 are considered aerobic [37]. The formula commonly used is

$$R = \frac{V_{CO_2}}{V_{O_2}} \tag{5}$$

in which V_{O2} and V_{CO2} are the body-mass-normalized, baseline subtracted, net volumes of oxygen and carbon dioxide exchanged during the activity period.

C. Steady State Metabolic Simulation

As an additional method of comparison, a simulation was performed in order to predict the steady state energy cost of stair ascent with each prosthesis. The time response of metabolic power to a step input in activity can be approximated as a first order function:

$$\dot{E}(t) = (\dot{E}_{SS} - \dot{E}(t_o))(1 - e^{-(t-t_0)/\tau}) + \dot{E}(t_o) \tag{6}$$

for time $t \geq t_0$, where E is net (baseline subtracted) metabolic energy and τ is the time constant. The subscript *ss* denotes steady state. Selinger and Donelan [38] showed this to be true for walking experiments. Assuming the same holds for stair ascent, which the data in Figures III-2 and III-3 appear to indicate, the steady state metabolic power can be predicted using the following formula if the time constant is known and the transient metabolic power is measured for at least one time constant:

$$\dot{E}_{SS} = \frac{\dot{E}(\tau+t_o)-\dot{E}(t_o)}{1-e^{-1}} + \dot{E}(t_o) \tag{7}$$

This model was applied to the metabolic data in order to predict what the steady state energy rate would be if the subjects had continued climbing long enough to reach it. It assumes the same time constant holds for each subject regardless of the prosthesis used. Time constants for each subject were determined using exponential best-fit curves, and the average value from all trials for a given subject was used in the analysis. The time constants ranged from 53-74 s, on the same order of magnitude as the 42 ± 12 s for healthy subject walking found by [38]. These time constants were used to estimate the steady state power for each trial. Steady state energy was estimated by multiplying the steady state power by the ascent time. Figure III-4 shows a plot with both the power calculated from the measured respiratory gases (black) and also the simulated power curve (blue). The yellow rectangle highlights the ascent period and has area proportional to the steady-state energy cost estimate.
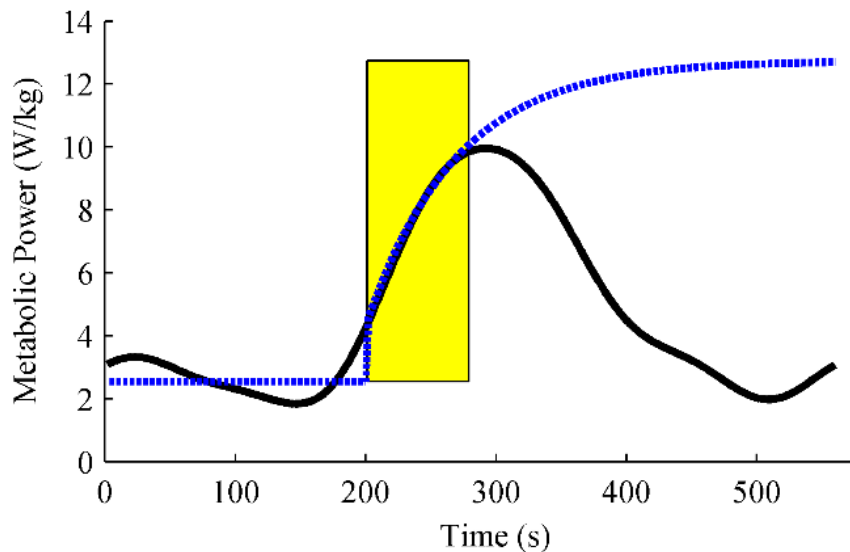
Figure III-4: Metabolic powers. The black curve represents power calculated from measured rates of O_2 and CO_2, while the dotted blue curve is the predicted first order response. The highlighted region shows the steady state energy estimate for the ascent period.

3. Results and Discussion

A. Joint Biomechanics

   The amputees ascended the stairs using a step-over gait with the powered prosthesis and a step-to gait with their passive ones. Data averaged over 10 consecutive strides for each subject, where the torque and power are body-mass-normalized, are shown in Figure III-5 for the knee (a) and ankle (b). The kinematics and kinetics obtained with the powered prosthesis are relatively close to healthy subject stair ascent gait reported by Riener et al. [17]. Although averaging dilutes the magnitude characteristics of individual stride data, the powered joints clearly exhibit several essential biomechanical features. The knee extensive torque and positive power in early stance (0-40 % stride), as the amputee mounts the step, are substantial. The average peak power achieved by the knee joint is 1.4 to 2.0 W/kg, approximately 62-90% of healthy. Although the torque and power peak slightly late, they still fall near the healthy envelope. At pushoff (40-60 % stride), the ankle torque dip is significant and the power shoots highly positive, though it peaks a bit earlier than the healthy norm. The average peak ankle joint power is 1.9 to 2.3 W/kg, approximately 75-92% of healthy. The knee angle beautifully nears healthy throughout the entire stride, and the ankle dorsiflexion in swing (60-100 % stride) enables step clearance. In all cases, net energy transfer for a stride was positive at each joint, corroborating the reduction seen in metabolic cost (see Section III-3-B).

19
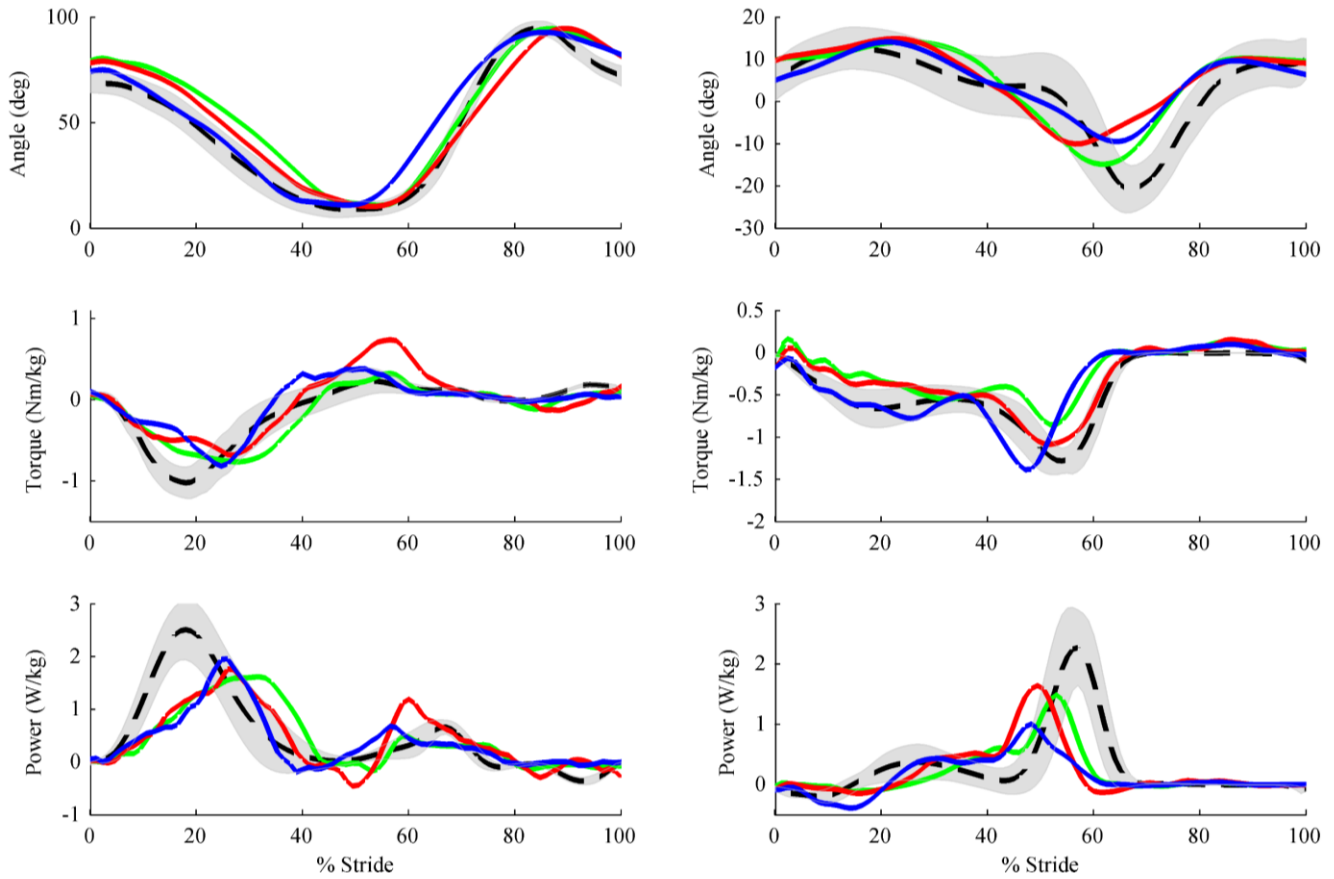
a) Knee joint

b) Ankle joint

Figure III-5: Joint biomechanics. The green, red and blue curves represent subjects 1, 2, and 3, respectively. The black dashed line shows the healthy average from [17], while the gray smear is ± one standard deviation.

Due to motor limitations and timing, the peak torques and powers do not quite reach healthy data in magnitude, although the shapes are similar. These torques and powers can only be achieved through proper controller tuning, using high gains, appropriate transition thresholds, and synchronizing joint motions. Furthermore, there is a tradeoff between kinematics and kinetics due to device limitations. The prosthesis can closely track a trajectory in the absence of external load, but then it would not transfer power. An example of this is late pushoff, in which case the ankle would plantarflex after the amputee's prosthetic foot was in the air. However, the motors are not strong enough to match certain desired joint kinematics when the prosthesis is fully weighted, resulting in lower velocities and powers. From Figure III-6, one can see that subject 3 (blue) has the lowest peak ankle power although his torque is still substantial. This is due to a premature pushoff.

One difference between the healthy and powered prosthesis data not shown in the figures is a slight pause exhibited by the amputees following foot strike of the prosthesis. This pause, comprising approximately 15% of stride, was due to each amputee's reluctance to fully trust a prosthesis with his weight, resulting in temporal asymmetry between steps with his two legs. Including the pause would artificially compress the powered prosthesis data relative to healthy, so it was omitted in order to minimize temporal distortion. If it were included, the prosthesis data in Figures III-5 and III-6 would extend an additional 15% beyond the healthy data, during which time the device is static.

B. *Transient Metabolics*

The transient metabolic energy expenditure, ascent time, and respiratory exchange ratio were averaged for each prosthesis condition over all four trials. On average, the amputees climbed 30% faster (a direct result of the ability to ascend reciprocally) and expended 24% less energy with the powered prosthesis than with their own daily use passive ones. Interestingly, the metabolic power was higher when climbing with the powered prosthesis, probably due to the quicker cadence. However, because the climb was significantly faster, total energy was lower. Comparisons of energy expenditures and ascent times across subjects are shown in Figures III-6 and III-7, and the metabolic and temporal results are given in Tables A-2 and A-4 in Appendix A as mean ± one standard deviation. Statistics for the filtered respiratory gas measurements are provided in Appendix B. From the graphs below, one can see that the means are clearly different, and standard deviations do not overlap between devices except for the ascent times of one subject. This anomaly is due to the fact that the first subject climbed faster at each session, so the first two trials with the powered prosthesis took longer than the last two trials with his daily use prosthesis.
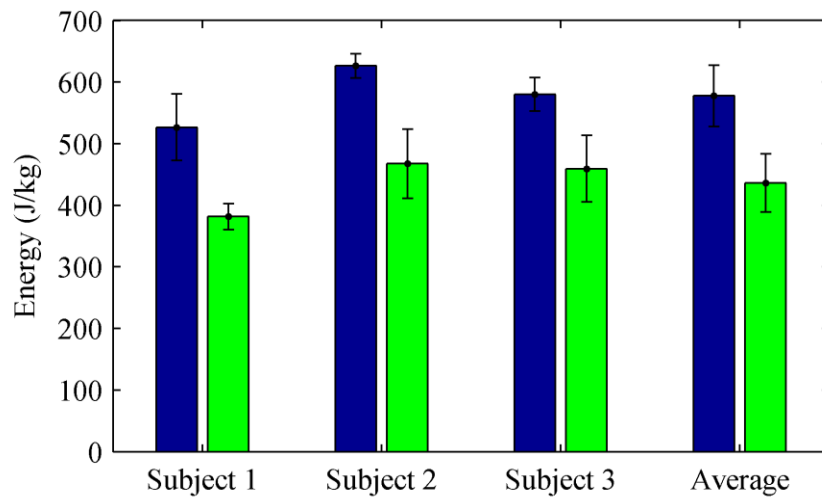
Figure III-6: Transient metabolic energy expenditures. Blue bars show averages for the passive prosthesis and green bars for the powered prosthesis. Error bars show $\pm$ one standard deviation.
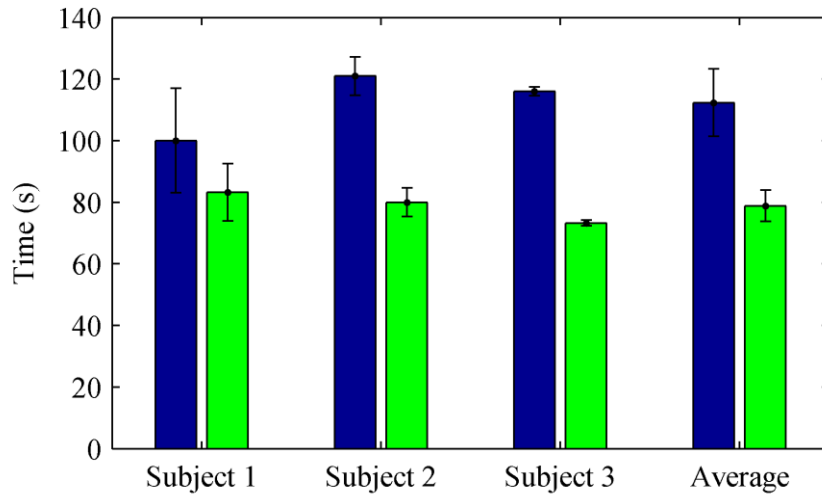
21

Figure III-7: Ascent times. Blue bars show averages for the passive prosthesis and green bars for the powered prosthesis. Error bars show $\pm$ one standard deviation.

Paired t-tests were run on energy expenditure and ascent time to compare the powered and passive cases. All results were statistically significant within 97% confidence for time and 99% confidence for energy. The p-values are summarized in Tables A-2 and A-4 in Appendix A. Although ascending stairs was certainly easier for these subjects with the powered prosthesis than with the passive one, these results do not necessarily extend to the entire transfemoral amputee population. The three subjects were all active males in their mid-forties. Amputees from a different demographic, particularly those who are weaker or heavier, could have different results.

Although none of the subjects had physical impairments in addition to their amputations, the second and third subjects were in better physical condition than the first. This is reflected in their respiratory exchange ratios. The average respiratory exchange ratio for Subject 1 is above 1.0, indicating anaerobic activity, and the ratios for the other two subjects are mostly below 0.9, showing borderline aerobic/anaerobic activity. This also reveals that climbing was more strenuous for the first subject than for the other two. These results are shown in Table III-2. The fact that R is nearly identical for the powered and passive cases with respect to each subject indicates that metabolic energy calculated from respiratory gases is an appropriate comparison metric.

Table III-2: Respiratory Exchange Ratio, R

Subject	$R_P \pm \sigma$	$R_0 \pm \sigma$
1	1.08 ± 0.08	1.14 ± 0.02
2	0.84 ± 0.04	0.84 ± 0.06
3	0.89 ± 0.07	0.88 ± 0.06
Avg.	0.93 ± 0.12	0.95 ± 0.15

The subscripts P and 0 represent the powered and passive prostheses, respectively.

C. Steady State Metabolics

Metabolic energy expenditure for ascending stairs at steady state was estimated for all trials. Results indicated that all subjects would still expend less energy using the powered prosthesis than their own passive ones if they had been climbing at steady state, as shown in Figure III-8. The powered prosthesis is predicted to require an average of 18% less energy than the passive ones with over 85% confidence for an individual and 99.99%

overall. These results are summarized in Table A-3 in Appendix A. While the energy savings predicted using this method are not as high as those calculated in the transient case, they are still substantial and confirm the trend of the measured results.
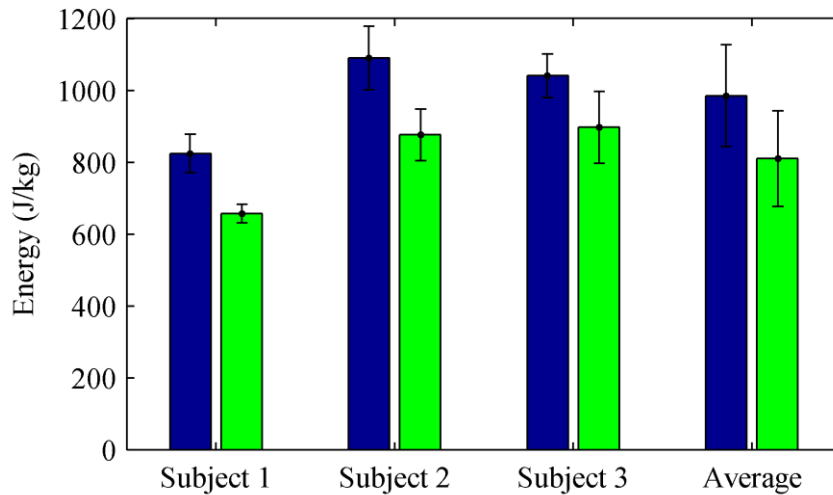

Figure III-8: Steady state energy expenditure prediction. Blue bars show averages for the passive prosthesis and green bars for the powered prosthesis. Error bars show ± one standard deviation.

Although there is no way to guarantee the accuracy of the predictions without extensive testing and much longer staircases, a comparison with literature provides reasonable confidence in the simulation. The estimated metabolic energy costs per meter ascent average 61.4 ± 8.5 J/(kg·m) and 50.6 ± 8.1 J/(kg·m) for the passive and powered conditions, respectively. These are near the average value of 52.5 ± 1.4 J/(kg·m) measured by Teh and Aziz [18] for healthy individuals ascending stairs at steady state, indicating that the predictions are reasonable. Furthermore, it shows that the amputees' energy expenditure is much closer to healthy when climbing with the powered prosthesis.

4. Conclusion

The powered prosthesis evaluated through the experiments on three amputee subjects described above shows a reduction in metabolic energy cost and ascent time and an improvement in joint biomechanics for stair ascent relative to passive prostheses. These results are expected due to the fact that a powered prosthesis can provide net positive energy transfer to the wearer, whereas a passive prosthesis does not. Specifically, using the fully powered prosthesis reduced the subjects' average energy expenditure by 24% and their ascent time by 30%, despite pausing after each step. The subjects were able to climb in a step-over manner with Vanderbilt's powered transfemoral prosthesis, but used a step-to gait with their own passive prostheses. Kinematics and kinetics obtained with the powered joints resembled healthy biomechanics. Furthermore, the subjects verbally expressed emphatic preferences for ascending stairs using the powered prosthesis rather than their own passive ones (see anecdotal evidence in Appendix F). This work demonstrates the effectiveness of a powered transfemoral prosthesis and controller in making stair ascent easier, faster and more natural for above-knee amputees, and it presents a method for metabolic analysis in the absence of steady state activity.

CHAPTER IV

EXPERIMENT 2: PARTIAL ASSISTANCE INVESTIGATION

1. Protocol

A second stair ascent experiment was conducted in which only the knee of the Vanderbilt prosthesis was actively controlled, hereafter referred to as the "mixed" condition. This was done to test the hypothesis that greater external power should correspond to lower effort by the user. The knee was chosen as the joint to power because it would enable reciprocal stair ascent, whereas the ankle has a minimal effect on this ability. The walking, standing, and stair descent controllers remained unchanged for this experiment.

In the partially powered condition, the knee was actively powered, while the ankle was controlled to behave passively. The control law used was the same as before. The knee used the same impedance parameters as in the fully powered case. The ankle equilibrium angle was commanded to be zero in every state, and the extra torque pulse was eliminated. The ankle spring stiffness was also kept constant, so no external power was introduced to this joint.

The experimental protocol and instrumentation were the same as for the previous experiment, with the exception that only two subjects (1 and 3) participated. After donning the metabolic apparatus and the prosthesis, each subject rested in his seat for 3 minutes. Then he rose, walked about 17 m to the stairwell, and ascended 79 steps. At the top, he turned and descended the stairs, and then walked back to his seat. After an additional 3 minute rest, he ended the test. Four trials were done for the partially powered condition, two each day with approximately 15 minutes rest in between them.

2. Results and Discussion

Analysis methods used were identical to those described previously. The mixed condition was compared to the passive and fully powered conditions from the original experiment. While the biomechanical results were uniform, the metabolic results for subjects 1 and 3 were quite different and will be individually discussed.

A. *Joint Biomechanics*

The amputees were able to ascend the stairs using a step-over gait for this experiment because the prosthetic knee was actively powered. Knee kinematics and kinetics are shown in Figure IV-1a. From the knee plots, it is clear that this joint is actively powered. The joint angle, torque, and power for each subject closely match healthy biomechanics from [17]. The most prominent features are the surges of torque and power in early stance, when the knee straightens to raise the amputee over the step. Average peak knee powers ranged from 79-86% of healthy.

Ankle kinematics and kinetics are visible in Figure IV-1b. These plots give evidence of the ankle's passivity, verifying that the controller functions as intended for this experiment. One can see that the ankle dorsiflexes in early stance, as the amputee loads the prosthesis, and it snaps to its equilibrium position of $0°$ when it is airborne during swing. There is clearly no dorsiflexion in late swing, no powered pushoff, and net energy transfer is approximately zero.

a) Knee joint   b) Ankle joint
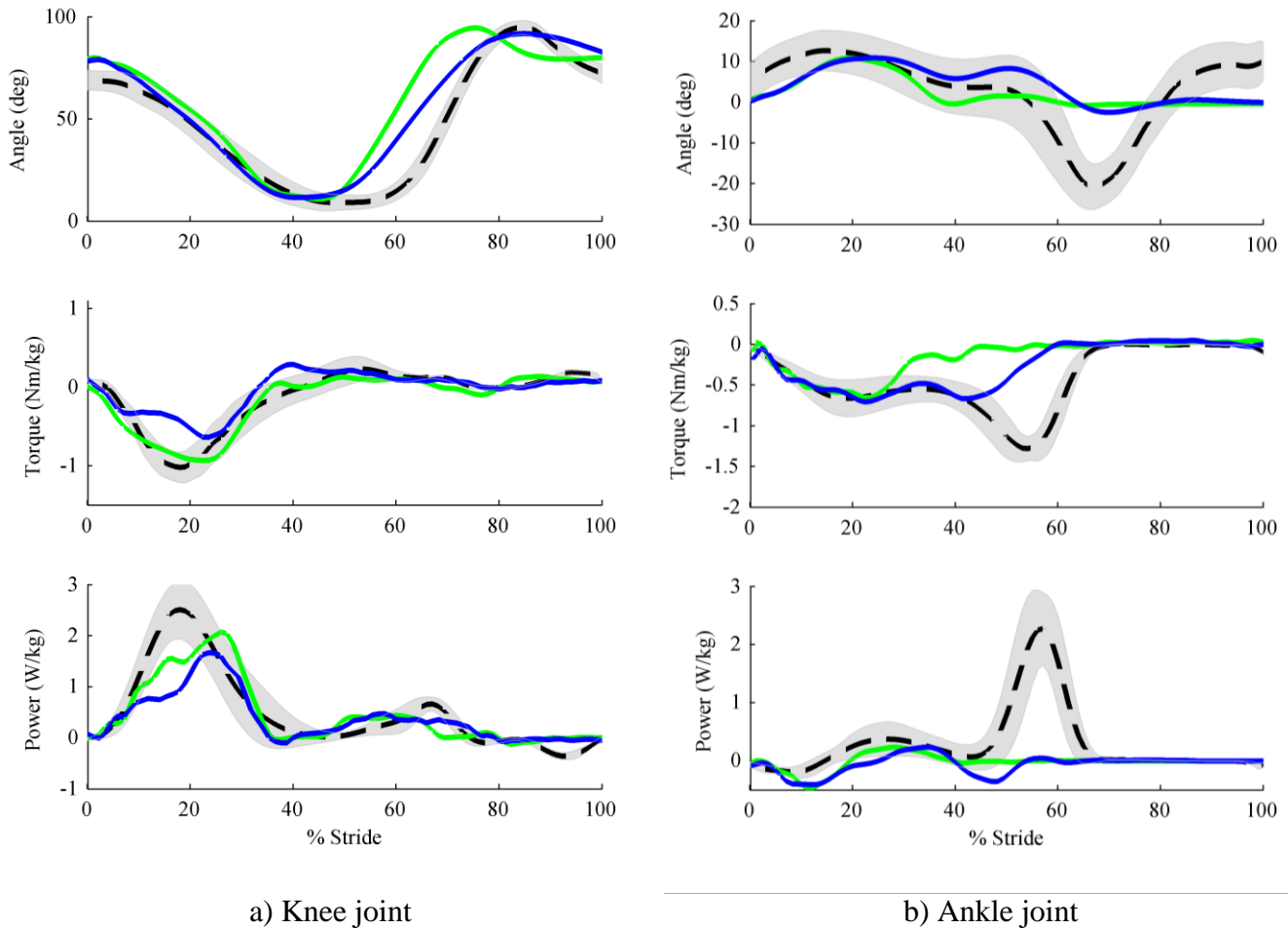
Figure IV-1: Joint biomechanics. The green and blue curves represent subjects 1 and 3, respectively. The black dashed line shows the healthy average from [17] while the gray smear is $\pm$ one standard deviation.

B. Metabolics

Results from Subject 1 supported the hypothesis that greater assistive power corresponds to lower effort required from the amputee. This subject used more energy to ascend stairs under the mixed condition than with the fully powered prosthesis, but less energy to ascend stairs than with his own passive prosthesis. The same held true for the steady state prediction.

Results from Subject 3 confirmed that powering the knee reduced the metabolic effort required to ascend stairs relative to using a passive prosthesis. However, results for the mixed condition and fully powered condition were not significantly different. It is important to note that of all three amputees, Subject 3 had the lowest power transfer from the ankle joint during the original experiment, thus the contribution of this joint was less significant. This may be why his metabolic results for the mixed condition are so similar to those of the fully powered condition.

Results for measured transient and predicted steady state energy expenditures are shown in Figures IV-2 and IV-3 below and detailed in Tables A-2 and A-3 in Appendix A. Although the results were not consistently statistically significant (see scattered p-values in Appendix A), the contribution of the powered joints in reducing metabolic effort is evident.

25

Figure IV-2: Transient energy expenditures. Blue bars show averages
for the passive, red for the mixed, and green for the fully powered
conditions. Error bars show $\pm$ one standard deviation.
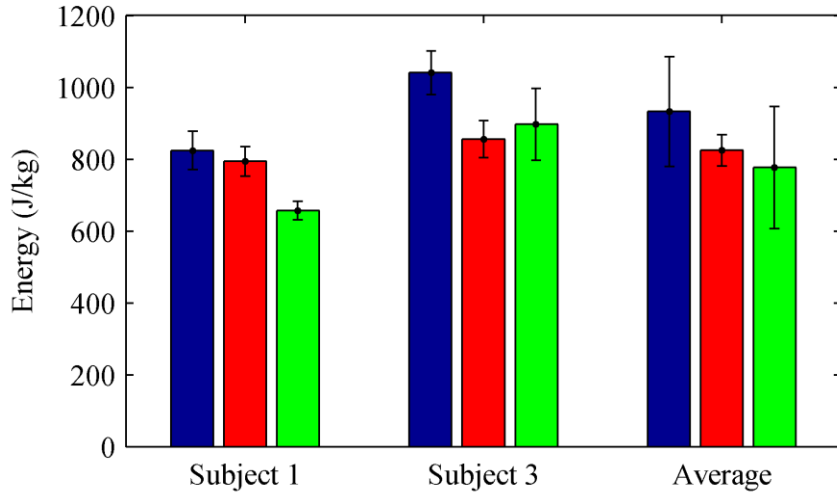
Figure IV-3: Steady state energy estimates. Blue bars show averages
for the passive, red for the mixed, and green for the fully powered
conditions. Error bars show $\pm$ one standard deviation.

Average ascent times for both subjects during this experiment were between their times for the fully powered and passive conditions. This is in line with the original hypothesis. While the standard deviations for Subject 1's ascent times overlap completely for the passive and mixed conditions, and the time difference is marginal, this may be due to the fact that Subject 1 completed this experiment approximately 10 weeks after the original one, and so was slightly out of practice using the Vanderbilt prosthesis. Bar graphs of the ascent times for all three conditions are shown in Figure IV-4, and statistics are detailed in Table A-4 in Appendix A.
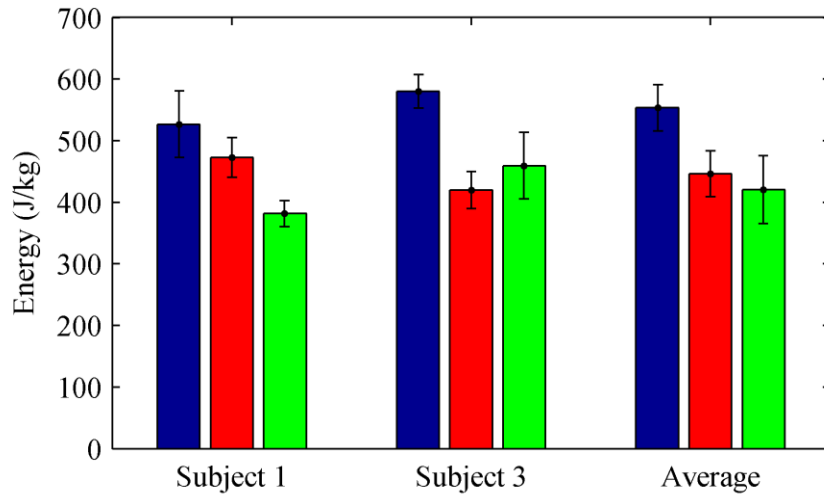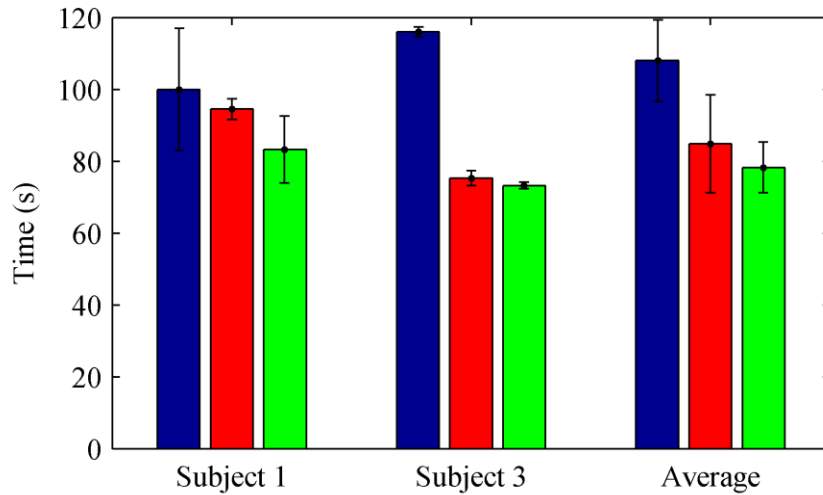
Figure IV-4: Ascent times. Blue bars show averages for the passive,
red for the mixed, and green for the fully powered conditions.
Error bars show ± one standard deviation.

Respiratory exchange ratio was just over 1.0 for Subject 1 and slightly below 0.9 for Subject 3, similarly to the original experiment. Thus changing the number of powered joints did not affect whether the activity was aerobic or anaerobic. As before, climbing stairs was anaerobic exercise for Subject 1 and borderline aerobic/anaerobic for Subject 3. These results are tabulated below.

Table IV-1: Respiratory Exchange Ratio, *R*

Subject	$R_H \pm \sigma$
1	1.04 ± 0.07
3	0.87 ± 0.02
Avg.	0.95 ± 0.10

3. Conclusion

This experiment did show that climbing stairs with a powered knee required less effort from both subjects than climbing with a passive one. It was also significantly faster. Therefore, the ability to ascend stairs using a step-over gait is a large gain energetically and temporally as well as biomechanically. The fact that the metabolic results for one subject under the fully powered and mixed cases were not significantly different indicates that normal knee function is more critical than normal ankle function for stair ascent.

APPENDICES

A. Metabolic Results Tables

Table A-1: Abbreviations Guide

Abbreviation	Meaning
0	passive prosthesis
CO_2	carbon dioxide
diff	difference
M	mixed condition
O_2	oxygen
P	powered prosthesis

Percent difference is given for the first subscript variable with respect to the second. For instance, in Table A-2, the negative energy difference for the powered prosthesis with respect to the passive one indicates lower energy expenditure for the powered condition.

Table A-2: Transient Metabolic Energy Statistics

Subject	$E_P \pm \sigma$ (J/kg)	$E_M \pm \sigma$ (J/kg)	$E_0 \pm \sigma$ (J/kg)	$diff_{P0}$ (%)	$diff_{M0}$ (%)	$diff_{MP}$ (%)	p_{P0}	p_{M0}	p_{MP}
1	382 ± 21	473 ± 32	527 ± 54	-28	-9	24	0.004	0.354	0.004
2	467 ± 57	--	627 ± 20	-25	--	--	0.006	--	--
3	460 ± 54	420 ± 30	580 ± 27	-21	-22	-9	0.010	0.007	0.262
Avg.	436 ± 58	446 ± 40	578 ± 54	-24	-19	6	$9.3*10^{-8}$	0.003	0.397

Table A-3: Steady State Metabolic Energy Statistics

Subject	τ (s)	$E_P \pm \sigma$ (W/kg)	$E_M \pm \sigma$ (J/kg)	$E_0 \pm \sigma$ (W/kg)	$diff_{P0}$ (%)	$diff_{M0}$ (%)	$diff_{MP}$ (%)	p_{P0}	p_{M0}	p_{MP}
1	53	662 ± 27	794 ± 41	824 ± 54	-20	-4	20	0.004	0.354	0.004
2	74	879 ± 74	--	1090 ± 88	-19	--	--	0.023	--	--
3	69	897 ± 99	890 ± 62	1041 ± 61	-14	-14	-1	0.122	0.026	0.489
Avg.	65	813 ± 130	842 ± 71	985 ± 136	-18	-10	8	$5.1*10^{-5}$	0.026	0.293

Table A-4: Ascent Time Statistics

Subject	$t_P \pm \sigma$ (s)	$t_M \pm \sigma$ (s)	$t_0 \pm \sigma$ (s)	$diff_{P0}$ (%)	$diff_{M0}$ (%)	$diff_{MP}$ (%)	p_{P0}	p_{M0}	p_{MP}
1	83 ± 9	95 ± 3	100 ± 17	-17	-6	14	0.024	0.511	0.053
2	80 ± 5	--	121 ± 6	-34	--	--	$3.7*10^{-4}$	--	--
3	73 ± 1	78 ± 2	116 ± 1	-37	-33	7	$1.8*10^{-5}$	$1.46*10^{-4}$	0.161
Avg.	79 ± 5	86 ± 9	112 ± 11	-30	-20	10	$2.9*10^{-6}$	0.018	0.033

B. Respiratory Gas Exchange Results

Table B-1: Abbreviations Guide

Abbreviation	Meaning
0	passive prosthesis
CO_2	carbon dioxide
diff	difference
M	mixed condition
O_2	oxygen
P	powered prosthesis

Net oxygen consumptions and carbon dioxide productions are tabulated below. Percent difference is given for the first subscript variable with respect to the second variable. For instance, in Table B-2, the negative oxygen difference for the powered prosthesis with respect to the passive one indicates lower oxygen consumption for the powered condition. Results indicate that, similarly to the transient energy calculations, respiratory gas exchanges are significantly lower for both the fully powered and mixed conditions than for the passive one. There is not a universal trend for the mixed condition versus the fully powered one.

Table B-2: Net O_2 Consumption Statistics

Subject	$O_{2P} \pm \sigma$ (mL/kg)	$O_{2M} \pm \sigma$ (mL/kg)	$O_{20} \pm \sigma$ (mL/kg)	$diff_{P0}$ (%)	$diff_{M0}$ (%)	$diff_{MP}$ (%)	p_{P0}	p_{M0}	p_{MP}
1	15.6 ± 0.9	19.2 ± 1.2	17.8 ± 1.4	-13	7	23	0.004	0.037	0.026
2	22.7 ± 2.5	--	26.8 ± 2.5	-16	--	--	0.006	--	--
3	22.4 ± 3.0	20.4 ± 1.5	24.2 ± 3.1	-8	-16	-9	0.010	0.004	0.052
Avg.	20.2 ± 4.0	19.8 ± 1.4	23.0 ± 4.6	-12	-6	7	$1.5*10^{-7}$	0.007	0.411

Table B-3: Net CO_2 Production Statistics

Subject	$CO_{2P} \pm \sigma$ (mL/kg)	$CO_{2M} \pm \sigma$ (mL/kg)	$CO_{20} \pm \sigma$ (mL/kg)	$diff_{P0}$ (%)	$diff_{M0}$ (%)	$diff_{MP}$ (%)	p_{P0}	p_{M0}	p_{MP}
1	16.6 ± 1.3	19.4 ± 1.2	19.9 ± 1.9	-17	-2	17	0.007	0.037	0.026
2	19.0 ± 2.7	--	22.0 ± 2.4	-14	--	--	0.024	--	--
3	19.7 ± 1.1	17.8 ± 1.5	21.0 ± 1.8	-6	-15	-10	0.008	0.004	0.052
Avg.	18.4 ± 2.2	18.6 ± 2.5	20.9 ± 2.1	-12	-9	4	$1.5*10^{-6}$	$2.3*10^{-4}$	0.426

Bar graphs of the net oxygen consumptions and carbon dioxide productions during both experiments are shown in Figures B-1 to B-4 below. Blue bars show averages for the passive, red for the mixed, and green for the fully powered conditions. Error bars show $\pm$ one standard deviation. The trends across devices are the same as for the transient energy results, which is believable since energy is proportional to a weighted sum of the net respiratory gases exchanged. Across subjects, the net CO_2 productions have closer values than do the O_2 consumptions. This explains why Subject 1's respiratory exchange ratio was higher than those of Subjects 2 and 3: his CO_2 production was similar, but his O_2 consumption was lower.
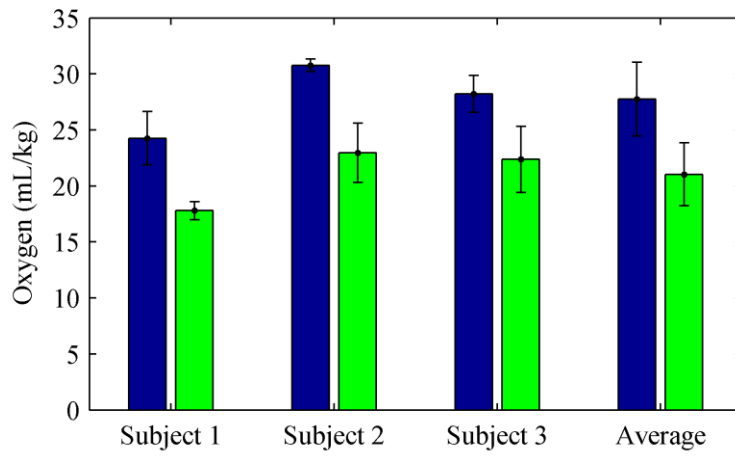
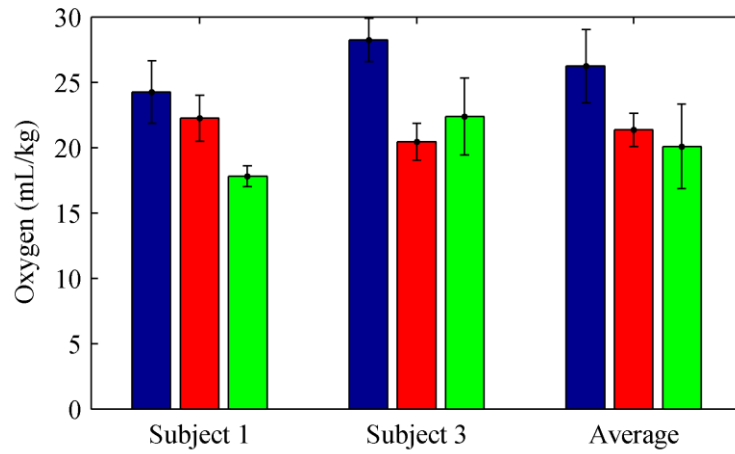Figure B-1: Net O$_2$ consumptions (Experiment 1).

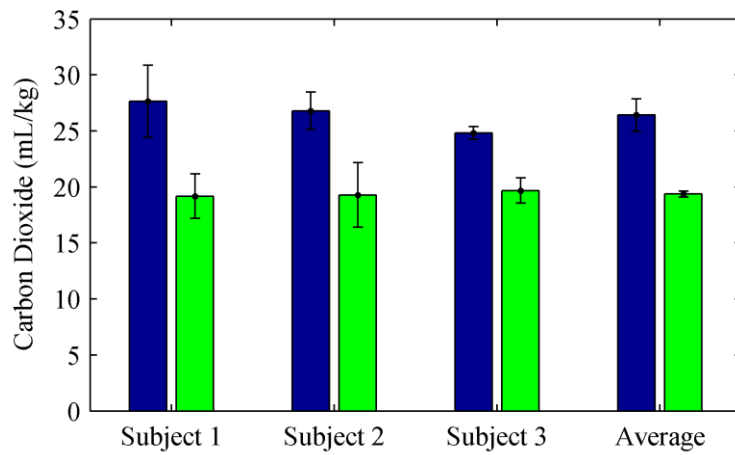
Figure B-2: Net O$_2$ consumptions (Experiment 2).

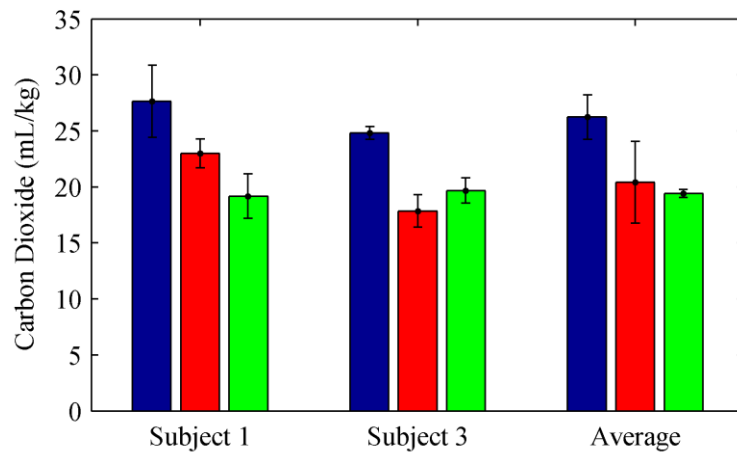Figure B-3: Net CO$_2$ productions (Experiment 1).

Figure B-4: Net CO_2 productions (Experiment 2).

C. Stair Ascent Controller Code

Below is the main code for the stair ascent controller. It is written in the C programming language in the MPLABX environment for implementation through Microchip PIC32 microcontrollers. Local functions and global variables are declared at the beginning. The governing state selection function (*smStairAscentHybrid*) is presented first. Then the torque generation functions (*genHybridStairAscentKneeTorque* and *genHybridStairAscentAnkleTorque*), which create the joint torque references from the impedance parameters and sensor signals, are listed. Next are the individual state functions (*s0_Straighten*, *s1_Rollover*, and *s2_Step*), described in Section II-2. Finally, a local function (*getSpline*) reads in position points from the subject's parameter file and computes derivatives for use in calculating the joint trajectory splines.

```c
//Copyright (c) 2014 Vanderbilt University
//All Rights Reserved.
//Note that the low-level code shown below reflects the philosophical description but
includes some differences due to implementation practicality.

#include "Pic32Main.h"
#include "Externals.h"
#include "CtrlStairHybrid.h"
#include "CtrlGeneral.h"

// Local scope function declarations
// ============================================================================
static void s0_Straighten(void);
static void s1_Rollover(void);
static void s2_Step(void);
static void getSpline(void);

// Global variables used only in CtrlStairAscentHybrid
// ============================================================================
static INT32 kXupst[SPLINE_POINTS_STAIR] = {0};
static INT32 kYupst[SPLINE_POINTS_STAIR] = {0};
static INT32 aXupst[SPLINE_POINTS_STAIR] = {0};
static INT32 aYupst[SPLINE_POINTS_STAIR] = {0};
static INT32 kY2upst[SPLINE_POINTS_STAIR] = {0};
static INT32 aY2upst[SPLINE_POINTS_STAIR] = {0};
static INT32 stepSizeUpst = 250;
static INT32 loadTimeUpst = 0;
static INT32 firstPushFlagUpst = 0;

// Overhead Function
// ============================================================================
void smStairAscentHybrid(void)
{
    if (gCON.mode.am_old != 6)
    {
        getSpline();
        gCON.mode.im = 2; // If new in hybrid stair ascent start in step
        firstPushFlagUpst = 1;
    }
    else
    {
        switch (gCON.mode.im_old)
        {
            case 0: // Straighten
                s0_Straighten();
                break;
```

32

```
            case 1: // Rollover
                s1_Rollover();
                break;
            case 2: // Step
                s2_Step();
                break;
            default: //if none of above are met
                gCON.mode.im = 2;
        }
    }
}


// Torque Generation Functions
// =============================================================================
void genHybridStairAscentKneeTorque(void)
{
    static INT32 KneeTorquePulse = 0;
    static INT32 Kndx = 0;
    static INT32 mode1Torque = 0;

    switch (gCON.mode.im)
    {
        case 0:
            gCON.kneeTorqueRef =
ImpCtrl(gHYBUPST.imped.knee_k[gCON.mode.im][gCON.mode.stm],
gHYBUPST.imped.knee_b[gCON.mode.im][gCON.mode.stm],
gHYBUPST.imped.knee_eq[gCON.mode.im][gCON.mode.stm], gDSS.KneePosFused.posFused,
gDSS.KneePosFused.encVel, KNEE_JOINT);
            Kndx = 0;
            break;
        case 1:
            gCON.kneeTorqueRef =
ImpCtrl(gHYBUPST.imped.knee_k[gCON.mode.im][gCON.mode.stm],
gHYBUPST.imped.knee_b[gCON.mode.im][gCON.mode.stm],
gHYBUPST.imped.knee_eq[gCON.mode.im][gCON.mode.stm], gDSS.KneePosFused.posFused,
gDSS.KneePosFused.encVel, KNEE_JOINT);
            Kndx = 0;
            mode1Torque = gCON.kneeTorqueRef;
            break;
        case 2:
            gCON.kneeTorqueRef =
ImpCtrl(gHYBUPST.imped.knee_k[gCON.mode.im][gCON.mode.stm],
gHYBUPST.imped.knee_b[gCON.mode.im][gCON.mode.stm],
gHYBUPST.imped.knee_eq[gCON.mode.im][gCON.mode.stm], gDSS.KneePosFused.posFused,
gDSS.KneePosFused.encVel, KNEE_JOINT);

            if (gRSS.load.lmf > 50000)        // safety condition for if someone trips and
catches himself with prosthesis side
            {
                gCON.kneeTorqueRef += mode1Torque;   // use mode 1 because mode 0 would
make leg straighten
            }

            break;
    }
}


void genHybridStairAscentAnkleTorque(void)
{
    static INT32 AnkleTorquePulse = 0;
    static INT32 Andx = 0;
```

```
    static INT32 mode0Torque = 0;

    switch (gCON.mode.im)
    {
        case 0:
            gCON.ankleTorqueRef =
ImpCtrl(gHYBUPST.imped.ankle_k[gCON.mode.im][gCON.mode.stm],
gHYBUPST.imped.ankle_b[gCON.mode.im][gCON.mode.stm],
gHYBUPST.imped.ankle_eq[gCON.mode.im][gCON.mode.stm], gDSS.AnklePosFused.posFused,
gDSS.AnklePosFused.encVel, ANKLE_JOINT);
            Andx = 0;
            mode0Torque = gCON.ankleTorqueRef;
            break;
        case 1:
            gCON.ankleTorqueRef =
ImpCtrl(gHYBUPST.imped.ankle_k[gCON.mode.im][gCON.mode.stm],
gHYBUPST.imped.ankle_b[gCON.mode.im][gCON.mode.stm],
gHYBUPST.imped.ankle_eq[gCON.mode.im][gCON.mode.stm], gDSS.AnklePosFused.posFused,
gDSS.AnklePosFused.encVel, ANKLE_JOINT);
            Andx = 0;

            break;
        case 2:
            gCON.ankleTorqueRef =
ImpCtrl(gHYBUPST.imped.ankle_k[gCON.mode.im][gCON.mode.stm],
gHYBUPST.imped.ankle_b[gCON.mode.im][gCON.mode.stm],
gHYBUPST.imped.ankle_eq[gCON.mode.im][gCON.mode.stm], gDSS.AnklePosFused.posFused,
gDSS.AnklePosFused.encVel, ANKLE_JOINT);

            if (gHYBUPST.anklePulseDuration==0) gHYBUPST.anklePulseDuration = 1;
            AnkleTorquePulse = (lcos32(Andx * SAMPLE_TIME * 360000 /
gHYBUPST.anklePulseDuration) / 1000000 - 1000) * gHYBUPST.anklePulsePeak / 2000;

            gCON.ankleTorqueRef -= AnkleTorquePulse;
            if ((Andx*SAMPLE_TIME) < gHYBUPST.anklePulseDuration) Andx++;
//          if (gRSS.load.lmf > 50000)      // safety condition for if someone trips
and catches himself with prosthesis side
//          {
//              gCON.ankleTorqueRef += mode0Torque;  // use mode 0 because mode 1 would
make ankle push off
//          }

            break;
    }
}

// Internal State Transition Functions
// =========================================================================
void s0_Straighten(void)
{
    static INT32 lTimer = 0;
    lTimer += 1;

    if (
            (gDSS.KneePosFused.posFused < gHYBUPST.thresh.knee_angle_thresh)
            &&
            (gDSS.AnklePosFused.posFused < gHYBUPST.thresh.ankle_angle_thresh)
            &&
            (gRSS.load.lmf > gHYBUPST.thresh.load_thresh))
    {
    //// if using s1 with separate pushoff:
```

34

```
        gCON.mode.im = 1;
        lTimer = 0;
            gCON.AnkleRateLim.eq.LimitBegin = 1;
            gCON.AnkleRateLim.eq.Time = 200;
                gCON.KneeRateLim.eq.LimitBegin = 1;
            gCON.KneeRateLim.eq.Time = 200;
    }
}


void s1_Rollover(void)
{
    static INT32 lTimer = 0;
    lTimer += 1;

    if  ((gRSS.load.lmf < gHYBUPST.thresh.deload_thresh)
            &&
         (lTimer >= 100))
    {
        gCON.mode.im = 2;
        stepSizeUpst = 100000*SAMPLE_TIME/gHYBUPST.trajTime;
        getSpline();
        lTimer = 0;
            gCON.KneeRateLim.eq.LimitBegin = 1;
            gCON.KneeRateLim.eq.Time = 200;
                gCON.AnkleRateLim.eq.LimitBegin = 1;
            gCON.AnkleRateLim.eq.Time = 200;
    }
}


void s2_Step(void)
{
    static INT32 lTimer = 0;
    static INT32 mprc = 0;   // millipercent of stride

    lTimer += 1;

    if (mprc <= 100000)
    {
        mprc += stepSizeUpst;  // increment mprc

        // interpolate spline position: calculate 5th argument (curve)
        splint(kXupst, kYupst, kY2upst, mprc, &gHYBUPST.imped.knee_eq[2][gCON.mode.stm]);
// & means find RAM address of subsequent variable
        splint(aXupst, aYupst, aY2upst, mprc,
&gHYBUPST.imped.ankle_eq[2][gCON.mode.stm]); // [1] means put new variable in 2nd spot of
that array
//         gHYBUPST.imped.ankle_eq[2][gCON.mode.stm] = 0;  // use for "passive" ankle
    }
    else if (
            (gRSS.load.lmf > gHYBUPST.thresh.load_thresh) // ensure weight is on stepping
foot
            &&
            (gDSS.AnklePosFused.posFused >
gHYBUPST.imped.ankle_eq[gCON.mode.im][gCON.mode.stm]))
    {
        firstPushFlagUpst = 0;
        gCON.mode.im = 0;
        gCON.KneeRateLim.eq.LimitBegin = 1;
      gCON.KneeRateLim.eq.Time = 500;
        gCON.AnkleRateLim.eq.LimitBegin = 1;
      gCON.AnkleRateLim.eq.Time = 500;
```

35

```
        mprc = 0;
        lTimer = 0;
    }
}


void getSpline(void)
{
    static INT32 kYP1 = 0;   // local variables for spline interp
    static INT32 aYP1 = 0;
    static INT32 kYPN = 0;
    static INT32 aYPN = 0;
    static INT32 i = 0;

    // get spline points from pegtfi
    for (i=0;i<SPLINE_POINTS_STAIR;i++)
        {
            kXupst[i] = gTRJst.kneeXref[gCON.mode.stm][i];
            kYupst[i] = gTRJst.kneeYref[gCON.mode.stm][i];
            aXupst[i] = gTRJst.ankleXref[gCON.mode.stm][i];
            aYupst[i] = gTRJst.ankleYref[gCON.mode.stm][i];
        }

    // ensure beginning knee position spline points are within range
    if      (gDSS.KneePosFused.posFused > MAX_TRAJ_KNEE_POS_STAIR)
        kYupst[0] = MAX_TRAJ_KNEE_POS_STAIR;
    else if (gDSS.KneePosFused.posFused < MIN_TRAJ_KNEE_POS_STAIR)
        kYupst[0] = MIN_TRAJ_KNEE_POS_STAIR;
    else     kYupst[0] = gDSS.KneePosFused.posFused;
    // specify initial ankle position
        aYupst[0] = gDSS.AnklePosFused.posFused;
    // set 1st derivatives of first and last knee position points = 0
    kYP1 = 0;
    kYPN = 0;
    // specify beginning range for ankle velocities
    if      (gDSS.AnklePosFused.encVel > MAX_TRAJ_ANKLE_VEL_STAIR)
        aYP1 = MAX_TRAJ_ANKLE_VEL_STAIR/stepSizeUpst*SAMPLE_TIME/1000;
    else if (gDSS.AnklePosFused.encVel < MIN_TRAJ_ANKLE_VEL)
        aYP1 = MIN_TRAJ_ANKLE_VEL_STAIR/stepSizeUpst*SAMPLE_TIME/1000;
    else     aYP1 = gDSS.AnklePosFused.encVel/stepSizeUpst*SAMPLE_TIME/1000;
    // make vector of positions and derivatives so computer can calculate spline easily
    // 1st 4 arguments are used to compute 5th
    spline(kXupst, kYupst, kYP1, kYPN, kY2upst);     //
[X(%swing),Y(deg),Y'first,Y'last,Y"]
    spline(aXupst, aYupst, aYP1, aYPN, aY2upst);     //
[X(%swing),Y(deg),Y'first,Y'last,Y"]
}
```

D. Metabolic Analysis Code

```matlab
function [ ErateSS,Energy,O2net,CO2net,tpeak] = calcMetabolicsFilt(
filename,tstart,tstop,type,m )
%CALCMETABOLICSFILT(filename,tstart,tstop,type,m) Calculates body-mass-normalized
%oxygen rate, energy rate, and energy expenditure.
%
%   This function calculates the body-mass-normalized rates of oxygen and
%   carbon dioxide gaseous exchange from spreadsheet data and uses them to
%   calculate net respiratory gas exchange and total energy expenditure
%   for an activity period.  Then it predicts steady state energy rate.
%   This function assumes at least a 3-minute initial rest period, which is
%   the subtracted baseline.  Finally, the gaseous exchange data is plotted
%   and numerical results are displayed.  This function can be edited to
%   only display the desired variables.
%
%   INPUTS:
%   filename: string with name of file
%   tstart: start time for activity
%   tstop: stop time for activity
%   type: prosthesis classification (powered or passive)
%   m: body mass (kg) of subject
%
%   OUTPUTS: for activity period
%   O2net: net oxygen consumption (mL/kg)
%   CO2net: net carbon dioxide production (mL/kg)
%   Energy: total energy expenditure (J/kg)
%   ErateSS: steady state energy expenditure rate (J/kgs)
%   tpeak: activity time (s)

% define energy equation
dEdt = @(VO2,VCO2) 16.58.*VO2 + 4.51.*VCO2; % Energy rate, J/s

% import data
[data text all] = xlsread(filename);
t = all(4:end,10);
time = mod(datenum(t,'HH:MM:SS'),1)*86400;  % time (s)
VO2 = data(4:end,14-1);        % oxygen consumption (mL/min)
VCO2 = data(4:end,15-1);       % carbon dioxide expiration (mL/min)
clearvars data text t

% convert gaseous exchange to mL/s
VO2 = VO2/60;
VCO2 = VCO2/60;

% median filter data to remove outliers
medpts = 5;      % filter window
O2mf = medfilt1(VO2,medpts);
CO2mf = medfilt1(VCO2,medpts);

% resample for even spacing
fs = 100;        % sampling frequency (Hz) use fs = 100
Ts = 1/fs;       % sample time (s)
trs = min(time):Ts:max(time); trs = trs';     % new time vector
O2rs = interp1(time,O2mf,trs);
CO2rs = interp1(time,CO2mf,trs);

% zero phase filter data
fc = .01;          % cutoff frequency (Hz) use fc = 0.01
```

```matlab
[O2zp,~,~] = ZeroPhaseFilter(O2rs,fs,fc);
[CO2zp,~,~] = ZeroPhaseFilter(CO2rs,fs,fc);

% downsample to improve computational speed
cutfactor = fs*2;
t = downsample(trs,cutfactor);
O2 = downsample(O2zp,cutfactor);
CO2 = downsample(CO2zp,cutfactor);

clearvars O2rs CO2rs O2mf CO2mf O2zp CO2zp trs

% find correct times
dEdt = dEdt(O2,CO2);   % calculate dE/dt
trise = tstop-tstart;
imax = find(dEdt==max(dEdt)); % index of peak energy rate
tmax = t(imax);             % time to peak
if(tstop<tmax)
    tstop = tmax;            % use longer t of peak or rise
end
tpeak = tmax-tstart;
% get start and stop indices of test
rest = find(t>=180); rest = rest(1);
start = find(t>=tstart); start = start(1);
stop = find(t>=tstop); stop = stop(1);

% calculate gas cost
O2_rest=mean(O2(1:rest));              % find avg O2 rate for baseline
VdotO2 = mean(O2(start:stop))-O2_rest; % calculate rate of O2 (mL/s)
O2net = VdotO2*(tstop-tstart);         % total oxygen volume (mL)
CO2_rest=mean(CO2(1:rest));            % find avg CO2 rate for baseline
VdotCO2 = mean(CO2(start:stop))-CO2_rest; % calculate rate of CO2 (mL/s)
CO2net = VdotCO2*(tstop-tstart);       % total oxygen volume (mL)

% calculate energy cost
Erate_rest=mean(dEdt(1:rest));         % find avg dE/dt for baseline
Erate_climb=mean(dEdt(start:stop));    % find avg dE/dt for activity
Erate=Erate_climb-Erate_rest;          % subtract baseline from activity
E=Erate*(tstop-tstart);                % calculate energy (J)
Erate_1 = dEdt(start);                 % energy rate at start of stairs

% estimate steady state energy
tau = 69;%45;   % metabolic time constant (s)
time_tau = find(t>=(tau+tstart)); time_tau = time_tau(1);
Erate_tau = dEdt(time_tau);
Erate_ss = (Erate_tau - Erate_1)/(1-exp(-1)) + Erate_1;
Erate_guess = (1-exp(-(t-tstart)/tau))*(Erate_ss-Erate_1) + Erate_1;
Erate_guess(1:start-1) = Erate_rest;
E_guess = (Erate_ss-Erate_rest)*(trise);

% plot gaseous exchange
figure()
hold on
rectangle('Position',[tstart,0,(tstop-tstart),max(VO2)/m],'FaceColor','y');
plot(time,VO2/m,'b.')
plot(t,O2/m,'k','LineWidth',2)
plot(time,VCO2/m,'r.')
plot(t,CO2/m,'k','LineWidth',2)
xlim([0 max(time)])
xlabel('Time (s)')
```

```matlab
ylabel('Gaseous Exchange Rates (\it{mL kg^-1 s^-1})')
title(sprintf('%s, VO_2 = %2.1f mL/kg, VCO_2 = %2.1f mL/kg, ErateSS = %2.2f J/kgs, t_a = 
%3.0f s', ...
    type,O2net/m,CO2net/m,(Erate_ss-Erate_rest)/m,tstop-tstart))
legend('VO_2 raw','VO_2 filt','VCO_2 raw','VCO_2 filt')

% plot energy rate
figure()
hold on
plot(t,dEdt/m,'g','LineWidth',2)
plot([tstart tstart],[0 max(dEdt)/m],'k:','LineWidth',2)
plot([tstop tstop],[0 max(dEdt)/m],'k:','LineWidth',2)
plot([trise+tstart trise+tstart],[0 max(dEdt)/m],'k:','LineWidth',2)
xlim([0 max(t)])
xlabel('Time (s)')
ylabel('Metabolic Power (W/kg)')
title('Energy Rate')

% plot energy rate guess
figure()
hold on
rectangle('Position',[tstart,Erate_rest/m,trise,(Erate_ss-
Erate_rest)/m],'FaceColor','y');
plot(t,dEdt/m,'k','LineWidth',2)
plot(t,Erate_guess/m,'b--','LineWidth',2)
xlabel('Time (s)')
ylabel('Metabolic Power (W/kg)')
title(sprintf('Ess Estimate %s, Eratess = %2.2f J/kgs, Ess = %4.0f J/kgs, t_a = %3.0f 
s',type,(Erate_ss-Erate_rest)/m,E_guess/m,tstop-tstart))

% body-mass-normalized outputs
Energy = E/m
ErateSS = (Erate_ss-Erate_rest)/m;
Erate/m;
O2net=O2net/m;
CO2net=CO2net/m;


end
```

E. Experiment 3: Protocol and Analysis Justification

In order to ensure that the amputee metabolic assessment was as fair and accurate as possible, it was necessary to justify some of the protocol and analysis selections. An experiment on a single healthy subject was performed to answer some important questions:
1) Does the ascent time adequately capture the comparative metabolic activity?
2) Is it necessary to rest at the top of the stairs rather than descending?
3) Does fixing cadence affect comparative results for different climbing techniques?

1. *Gait and Cadence Experiment*

The subject climbed on the same staircase and wore the same K4b^2 metabolic apparatus as the amputees, described in Chapter III: Experiment 1. Three different gait conditions were tested: a step-to gait at a fixed cadence, a step-over gait at the same fixed cadence, and a step-over gait at a self-selected pace. The fixed cadence was 1 step/s, which is approximately the speed of the amputees climbing with the powered prosthesis, and as fast as the healthy subject could reasonably climb with a step-to gait. A stopwatch was used to time each trial and regulate the fixed cadence conditions.

The experiment began with the subject resting at the base of the staircase for three minutes. Then she ascended 79 stairs using one of the gait techniques described. At the top, she remained standing until 8 minutes had elapsed since the start, during which time she returned to her resting metabolic baseline. After an additional 10 minute rest, she repeated the experiment twice, under each of the other two climbing conditions. The complete experiment was conducted on three separate days. The order of test conditions was rotated so that each trial had a turn to be first, second, and third.

2. *Analysis*

Baseline subtracted metabolic power and energy were calculated for each trial using the methods in Chapter III: Experiment 1. Four different analysis times were used: rise time t_r, peak time t_p, settling time t_s, and end time t_e. These are indicated in Figure E-1 and described in Table E-1.
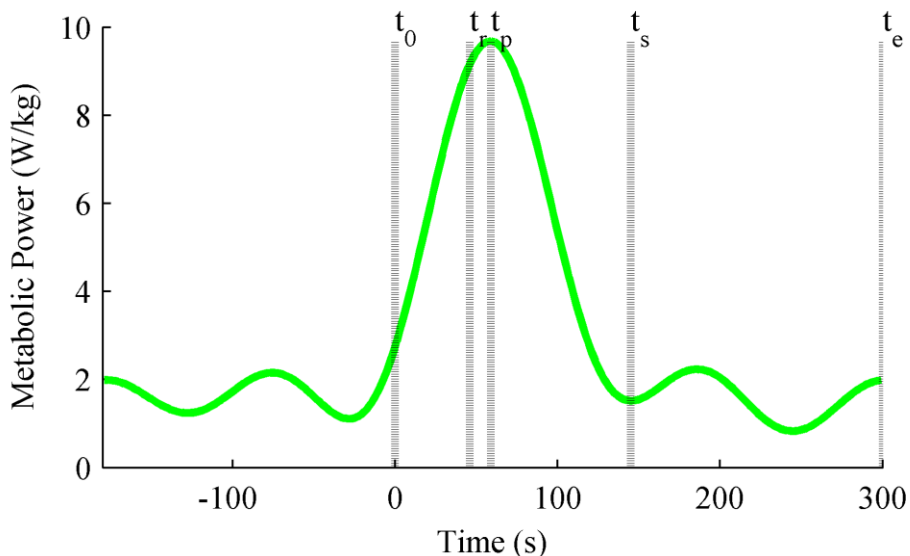

Figure E-1: Metabolic power with time indications. The dotted vertical lines represent (from left to right) start time, rise time, peak time, settling time, and end time.

Table E-1: Experimental Analysis Times

Time	Description
t_r	Time to summit
t_p	Time to peak energy rate
t_s	Time to return to baseline
t_e	Time test ended

The rise and end times were measured directly, the peak time was algorithmically determined, and the settling time was found manually.

3. Results and Discussion

The times and the metabolic energies and powers calculated through measured respiratory gases are shown in figures E-2, E-3, and E-4. The step-over self-selected cadence was, on average, 44% faster than the fixed cadence of 1 step/s. Depending on the analysis times, the energy calculated through respiratory gas measurements was 22-55% less for the step-over self-selected pace and 14-18% less for the step-over fixed pace than for the step-to gait.
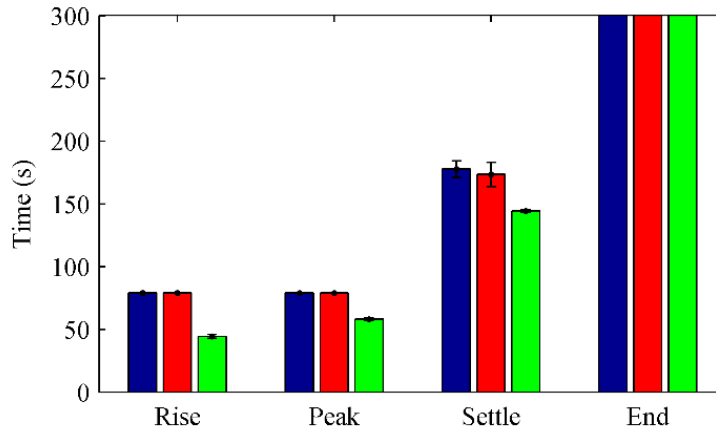

Figure E-2: Analysis times. Blue bars show averages for the step-to gait, red for the fixed step-over gait, and green for the self-selected step-over gait. Error bars show ± one standard deviation.

Figure E-3: Metabolic energy. Blue bars show averages for the step-to gait, red for the fixed step-over gait, and green for the self-selected step-over gait. Error bars show ± one standard deviation.

Figure E-4: Metabolic power. Blue bars show averages for the step-to gait, red for the fixed step-over gait, and green for the self-selected step-over gait. Error bars show $\pm$ one standard deviation.
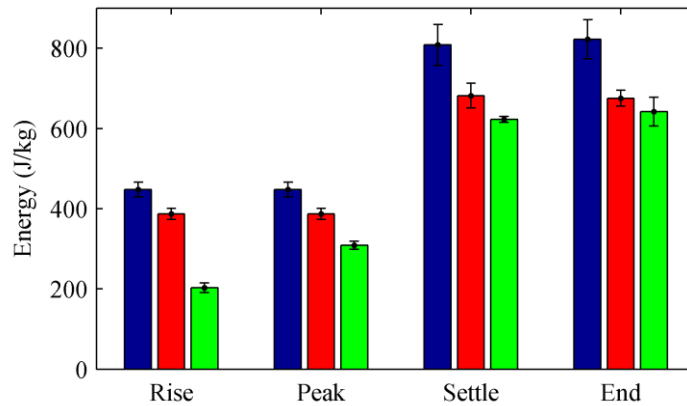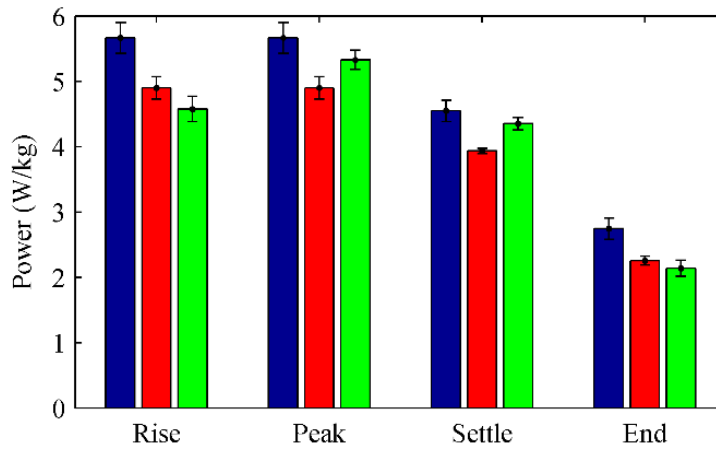
For the fixed cadence conditions, rise time and peak time were identical. For the third condition, the peak energy rate was about 32% after the subject reached the summit, indicating catch-up metabolic effects continuing after climbing ceased. Therefore, the energy expenditure determined by the peak time for this case was greater than the one found using the rise time. This answered the first question: using rise time does not always adequately capture the metabolic effort required for ascent. For this reason, peak time is a better option if the peak energy rate occurs after the subject reaches the top of the stairs.

The fact that the energies for settling and end time are nearly identical indicate that the manual selections for settling time were accurate. In comparing the metabolic energies and powers for the peak and settling times, it is clear that the comparative results are quite similar. Average powers trends are nearly identical for each condition. The settling time energy is roughly twice the peak time energy for each condition, and the relative results are similar. This answers the second question: peak time captures relative metabolic effort results similarly to settling time, so peak time is an appropriate analysis tool. Thus, the subjects do not need to stop at the top of the stairs to rest, and descending is permissible.

Regardless of analysis time, overall trends are clear. The step-over gait at a self-selected cadence is the most metabolically efficient, followed by the step-over gait at a fixed cadence, while the step-to gait is the hardest. A step-over gait also enables faster climbing. Although the metabolic power was lower for the fixed cadence step-over gait than the self-selected cadence, the overall energy expenditure was still higher due to the longer analysis time. This answers the third question: fixing cadence does affect relative results. Therefore it is ideal for subjects to self-select their cadence for the most accurate comparison of metabolic effort.

F. User Testimonials

All three transfemoral amputee subjects preferred to ascend stairs using the powered prosthesis as opposed to their own passive daily use devices. Following are some anecdotes regarding their experience:

Subject 1 claimed that using his C-leg requires much more exertion and that climbing with the powered prosthesis is much less tiring, professing:
"It's like a covered wagon versus a Cadillac."

Subject 2 was quite enthusiastic and prolific with positive comments:
- "The bottom line is, the robot leg is easier to climb with than a passive leg."
- "I know scientifically, it doesn't mean [s**t], but being able to climb up and down stairs like a normal person is night and day difference. That little split-second of extra transition time is worth the ease. That robot leg is amazing."
- "Let me tell you, another thing that robot leg is good for, over the years, is saving your good leg. The fatigue is night and day difference."

Subject 3 enjoyed his renewed ability to ascend stairs step-over-step, stating:
"The robot leg, once I learned to let it work for me, simplified ascending stairs very similarly to pre-amputation ease."

REFERENCES

[1]   K. Ziegler-Graham, E. J. MacKenzie, P. L. Ephraim, T. G. Travison, and R. Brookmeyer, "Estimating the prevalence of limb loss in the United States: 2005 to 2050," *Archives of physical medicine and rehabilitation,* vol. 89, pp. 422-429, 2008.

[2]   D. G. Smith. (2004) The Transfemoral Amputation Level, Part 1: "Doc, It's Ten Times More Difficult!". *inMotion*. Available: http://www.amputee-coalition.org/inmotion/mar_apr_04/transfemoral.html

[3]   P. G. Adamczyk and A. D. Kuo, "Mechanisms of Gait Asymmetry Due to Push-Off Deficiency in Unilateral Amputees," *TNSRE,* vol. 23, pp. 776-785, 2014.

[4]   R. Waters, J. Perry, D. Antonelli, and H. Hislop, "Energy cost of walking of amputees: the influence of level of amputation," *The Journal of Bone & Joint Surgery,* vol. 58, pp. 42-46, 1976.

[5]   E. D. Ledoux, B. E. Lawson, A. H. Shultz, H. L. Bartlett, and M. Goldfarb, "Metabolics of Stair Ascent with a Powered Transfemoral Prosthesis," presented at the IEEE EMBC, 2015.

[6]   E. Ledoux and M. Goldfarb, "Control and Evaluation of a Powered Transfemoral Prosthesis for Stair Ascent," *TNSRE,* submitted for publication 7/5/2016.

[7]   C. D. Hoover, G. D. Fulk, and K. B. Fite, "Stair ascent with a powered transfemoral prosthesis under direct myoelectric control," *Mechatronics, IEEE/ASME Transactions on,* vol. 18, pp. 1191-1200, 2013.

[8]   B. E. Lawson, H. A. Varol, A. Huff, E. Erdemir, and M. Goldfarb, "Control of stair ascent and descent with a powered transfemoral prosthesis," *Neural Systems and Rehabilitation Engineering, IEEE Transactions on,* vol. 21, pp. 466-473, 2013.

[9]   T. Lenzi, J. Sensinger, J. Lipsey, L. Hargrove, and T. Kuiken, "Design and preliminary testing of the RIC hybrid knee prosthesis," in *2015 37th Annual International Conference of the IEEE Engineering in Medicine and Biology Society (EMBC)*, 2015, pp. 1683-1686.

[10]   G. R. Colborne, S. Naumann, P. E. Longmuir, and D. Berbrayer, "Analysis of Mechanical and Metabolic Factors in the Gait of Congenital Below Knee Amputees: A Comparison of the SACH and Seattle Feet," *American Journal of Physical Medicine & Rehabilitation,* vol. 71, pp. 272-278, 1992.

[11]   S. K. Au, J. Weber, and H. Herr, "Powered Ankle--Foot Prosthesis Improves Walking Metabolic Economy," *Robotics, IEEE Transactions on,* vol. 25, pp. 51-66, 2009.

[12]   G. Traugh, P. Corcoran, and R. Reyes, "Energy expenditure of ambulation in patients with above-knee amputations," *Archives of physical medicine and rehabilitation,* vol. 56, pp. 67-71, 1975.

[13]   M. Taylor, E. Clark, E. Offord, and C. Baxter, "A comparison of energy expenditure by a high level trans-femoral amputee using the Intelligent Prosthesis and conventionally damped prosthetic limbs," *Prosthetics and Orthotics International,* vol. 20, pp. 116-121, 1996.

[14]   D. Datta, B. Heller, and J. Howitt, "A comparative evaluation of oxygen consumption and gait pattern in amputees using Intelligent Prostheses and conventionally damped knee swing-phase control," *Clinical rehabilitation,* vol. 19, pp. 398-403, 2005.

[15]   C. Huang, J. Jackson, N. Moore, P. Fine, K. Kuhlemeier, G. Traugh, and P. Saunders, "Amputation: energy cost of ambulation," *Archives of physical medicine and rehabilitation,* vol. 60, pp. 18-24, 1979.

[16]   M. Traballesi, P. Porcacchia, T. Averna, and S. Brunelli, "Energy cost of walking measurements in subjects with lower limb amputations: a comparison study between floor and treadmill test," *Gait & posture,* vol. 27, pp. 70-75, 2008.

[17]   R. Riener, M. Rabuffetti, and C. Frigo, "Stair ascent and descent at different inclinations," *Gait & posture,* vol. 15, pp. 32-44, 2002.

[18]   K. C. Teh and A. R. Aziz, "Heart rate, oxygen uptake, and energy cost of ascending and descending the stairs," *Medicine and science in sports and exercise,* vol. 34, pp. 695-699, 2002.

[19]   E. R. O'Connell, P. C. Thomas, L. D. Cady, and R. J. Karwasky, "Energy costs of simulated stair climbing as a job-related task in fire fighting," *Journal of Occupational and Environmental Medicine,* vol. 28, pp. 282-284, 1986.

[20]   J. S. Gottschall, G. S. Aghazarian, and E. A. Rohrbach, "The metabolic and muscular differences between two stair-climbing strategies of young adults," *The Journal of Strength & Conditioning Research,* vol. 24, pp. 2558-2563, 2010.

[21]   Ossur, "Proprio Foot Technical Manual," ed: Ossur, 2013, pp. 1-19.

[22]   BionX. (2016). *The BiOM Advantage*. Available: http://www.bionxmed.com/patients/the-biom-advantage/

[23]   H. M. Herr and A. M. Grabowski, "Bionic ankle–foot prosthesis normalizes walking gait for persons with leg amputation," *Proceedings of the Royal Society of London B: Biological Sciences,* vol. 279, pp. 457-464, 2012.

[24]   O. Bock, "Quick Guide #3: C-Leg Patient Training Overview," O. Bock, Ed., ed, 2006.

[25]   O. Bock. *C-Leg Product Page*. Available: https://professionals.ottobockus.com/zb2b4ob/us01/en/USD/Prosthetics/Lower-Limb-Prosthetics/Knees--Microprocessor/C-Leg/C-Leg/p/3C88-3~59~82

[26]   O. Bock and K. B. James, "System for controlling artifical knee joint action in an above knee prosthesis," 0549855A2, 1993.

[27]   Ossur, "Rheo Knee 3," Ossur Catalog ed, 2016, pp. 73-76.

[28]   F. Innovations, "Plie 3 MPC Knee," ed: Freedom Innovations, 2015, pp. 62-65.

[29]   O. Bock, "Genium X3," O. Bock, Ed., ed, 2013.

[30]   Orthomobility. (2016). *Very Good Knee (VGK)*. Available: http://www.orthomobility.com/

[31]   Ossur, "Power Knee," Ossur, Ed., Ossur Americas Prosthetics Catalog ed, pp. 20-23.

[32]   Ossur, "Power Knee Quick Reference Card," Ossur, Ed., ed, 2013.

[33]   B. E. Lawson, J. Mitchell, D. Truex, A. Shultz, E. Ledoux, and M. Goldfarb, "A Robotic Leg Prosthesis: Design, Control, and Implementation," *Robotics & Automation Magazine, IEEE,* vol. 21, pp. 70-81, 2014.

[34]   B. E. Lawson, H. A. Varol, and M. Goldfarb, "Ground adaptive standing controller for a powered transfemoral prosthesis," in *Rehabilitation Robotics (ICORR), 2011 IEEE International Conference on*, 2011, pp. 1-6.

[35]   D. A. Winter, "Kinematic and kinetic patterns in human gait: variability and compensating effects," *Human Movement Science,* vol. 3, pp. 51-76, 1984.

[36]   J. Brockway, "Derivation of formulae used to calculate energy expenditure in man," *Human nutrition. Clinical nutrition,* vol. 41, pp. 463-471, 1987.

[37]   E. E. M. da Rocha, V. G. F. Alves, and R. B. V. da Fonseca, "Indirect calorimetry: methodology, instruments and clinical application," *Current Opinion in Clinical Nutrition & Metabolic Care,* vol. 9, pp. 247-256, 2006.

[38]   J. C. Selinger and J. M. Donelan, "Estimating instantaneous energetic cost during non-steady-state gait," *Journal of Applied Physiology,* vol. 117, pp. 1406-1415, 2014.